EBioMedicine 71 (2021) 103570

Contents lists available at ScienceDirect

EBioMedicine

journal homepage: www.elsevier.com/locate/ebiom

Dynamics and epigenetic signature of regulatory T-cells following antiretroviral therapy initiation in acute HIV infection

Alexis Yero[1], Tao Shi[1], Omar Farnos[1], Jean-Pierre Routy[2,3], Cécile Tremblay[4,5], Madeleine Durand[4], Christos Tsoukas[2,6], Cecilia T. Costiniuk[2,7], Mohammad-Ali Jenabian[1,5,7,*]

[1] Department of Biological Sciences and CERMO-FC Research Centre, Université du Québec à Montréal (UQAM), Montreal, QC, Canada
[2] Research Institute of McGill University Health Centre, Montreal, QC, Canada
[3] Chronic Viral Illness Service, Division of Infectious Disease, Department of Medicine, Glen Site, McGill University Health Centre, Montreal, QC, Canada
[4] CHUM Research Centre, Montreal, QC, Canada
[5] Department of Microbiology, Infectiology and Immunology, Faculty of Medicine, Université de Montréal, Montreal, QC, Canada
[6] Division of Clinical Immunology and Allergy, Faculty of Medicine, McGill University, Montreal, QC, Canada
[7] Department of Microbiology & Immunology, McGill University, Montreal, QC, Canada

ARTICLE INFO

Article History:
Received 27 May 2021
Revised 10 August 2021
Accepted 19 August 2021
Available online xxx

Keywords:
HIV
antiretroviral therapy (ART)
regulatory T-cells (Tregs)
FoxP3
TGF-β1
CD39

ABSTRACT

Background: HIV infection promotes the expansion of immunosuppressive regulatory T-cells (Tregs), contributing to immune dysfunction, tissue fibrosis and disease progression. Early antiretroviral treatment (ART) upon HIV infection improves CD4 count and decreases immune activation. However, Treg dynamics and their epigenetic regulation following early ART initiation remain understudied.

Methods: Treg subsets were characterized by flow cytometry in 103 individuals, including untreated HIV-infected participants in acute and chronic phases, ART-treated in early infection, elite controllers (ECs), immunological controllers (ICs), and HIV-uninfected controls. The methylation status of six regulatory regions of the *foxp3* gene was assessed using MiSeq technology.

Findings: Total Treg frequency increased overtime during HIV infection, which was normalized in early ART recipients. Tregs in untreated individuals expressed higher levels of activation and immunosuppressive markers (CD39, and LAP(TGF-β1)), which remained unchanged following early ART. Expression of gut migration markers (CCR9, Integrin-β7) by Tregs was elevated during untreated HIV infection, while they declined with the duration of ART but not upon early ART initiation. Notably, gut-homing Tregs expressing LAP(TGF-β1) and CD39 remained higher despite early treatment. Additionally, the increase in LAP(TGF-β1)$^+$ Tregs overtime were consistent with higher demethylation of conserved non-coding sequence (CNS)-1 in the *foxp3* gene. Remarkably, LAP(TGF-β1)-expressing Tregs in ECs were significantly higher than in uninfected subjects, while the markers of Treg activation and gut migration were not different.

Interpretation: Early ART initiation was unable to control the levels of immunosuppressive Treg subsets and their gut migration potential, which could ultimately contribute to gut tissue fibrosis and HIV disease progression.

Funding: This study was funded by the Canadian Institutes of Health Research (CIHR, grant MOP 142294) and in part by the AIDS and Infectious Diseases Network of the *Réseau SIDA et maladies infectieuses du Fonds de recherche du Québec-Santé* (FRQ-S).

1. Introduction

Regulatory T-cells (Tregs) consist of a subset of CD4 T-cells with immunosuppressive functions that expresses high levels of CD25 (α chain of IL-2 receptor), low levels of CD127 (α chain of IL-7 receptor), and the master transcription factor forkhead box P3 (FoxP3) which controls Treg lineage stability and immunosuppressive functions [1-3]. Tregs can be further classified into thymic Tregs (tTregs) and peripheral Tregs (pTregs), depending on their site of differentiation. tTregs are generated from CD4 and CD8 double-positive thymocytes upon recognition of self-antigens, and they constitute the majority of circulating Tregs in lymphoid organs and peripheral blood [1-3]. On the other hand, pTregs are differentiated from circulating naïve CD4 T-cells under inflammatory conditions in the presence of IL-2 and transforming growth factor-beta 1 (TGF-β1). pTregs are more prevalent in certain organs, such as the

* Corresponding author: Mohammad-Ali Jenabian, DVM, PhD; Department of Biological Sciences, Université du Québec à Montréal (UQAM). Address: 141, Avenue President Kennedy, Room SB3385, Montreal (QC) Canada, H2 X 1Y4. Tel: +1 (514) 987-3000, Ext. 6794; Fax: +1 (514) 987-4647
E-mail address: jenabian.mohammad-ali@uqam.ca (M.-A. Jenabian).

https://doi.org/10.1016/j.ebiom.2021.103570

Research in Context

Evidence before this study

Early HIV infection is characterized by rapid CD4 T-cell depletion, a dramatic increase in immune activation, and irreversible gut mucosal fibrosis, which are associated with increased frequencies of immunosuppressive regulatory T-cells (Tregs). Tregs contribute to HIV disease progression by promoting immune dysfunction and tissue fibrosis. Antiretroviral therapy (ART) initiation as early as possible is recommended to decrease HIV burden, immune dysfunction, and secondary HIV transmission. However, ART is unable to restore gut mucosal integrity, and such mucosal damage is present even in individuals that naturally control HIV viral replication, known as elite controllers (ECs). The impact of early ART initiation during acute HIV infection on Tregs subset dynamics remains understudied.

Added value of this study

Herein, we assessed the dynamics of various Treg subsets in HIV-infected individuals with different clinical outcomes and after early ART initiation. We found that, despite decreasing total Tregs frequencies, early ART initiation was unable to normalize the proportion of immunosuppressive Treg subsets, including $CD39^+$, and $LAP(TGF\text{-}\beta1)^+$ Tregs, and their potential to migrate toward the gut. Importantly, we showed that even in ECs, the frequencies of pro-fibrotic Tregs ($LAP(TGF\text{-}\beta1)^+$) Tregs and their migration into the gut was higher than in uninfected individuals, which support previous reports on gut fibrosis in ECs. Additionally, for the first time, we evaluated the epigenetic regulation of six major regions of the *foxp3* gene, the master regulator of Treg suppressive functions. We found increased demethylation of conserved non-coding sequences (CNS) 1 in the *foxp3* gene, which is known to be induced by TGF-β1.

Implications of all the available evidence

Our findings fill a knowledge gap on progressive and irreversible gut fibrosis mechanisms despite early ART initiation. Our results highlight the role of pro-fibrogenic Tregs via CD39/TGF-β1 pathway and their homing in the gut despite early ART. These observations underscore Tregs as potential targets for HIV immunotherapeutic interventions in combination with ART.

gut, where they prevent local inflammation and establish tolerance against exogenous antigens [1-3].

Conserved non-coding sequences (CNSs) within the *foxp3* locus are involved in Treg lineage stability and subsequent suppressive functions. DNA demethylation of CNS1 and CNS2 are required for the differentiation of pTregs and tTregs, respectively [4]. The binding of Smad2/3 to CNS1 induced by TGF-β signaling is critical for pTreg cell differentiation [5]. CNS2, also known as the Treg-specific demethylated region (TSDR), is highly enriched in CpG sites which are fully demethylated only in tTregs, contributing to the maintenance of FoxP3 expression and tTreg lineage stability [6]. Another intronic regulatory element, CNS3, plays an important role in expanding both tTreg and pTreg cells, and it is suggested that CNS3 lowers the threshold of the T-cell receptor (TCR) signaling strength and potentiates the transcription of FoxP3[7,8]. Chronic HIV infection is associated with increases in the proportion of Tregs and their activation in both acute and chronic stages, which play a deleterious role during the infection by decreasing HIV-specific immune responses, T-cell proliferation, and cytokine production, and promoting viral persistence [2,9-11]. Importantly, Tregs in the colon mucosa and peripheral blood of HIV-infected individuals demonstrate higher demethylation in the *foxp3* promoter compared to those of healthy controls, indicating an enhanced function [12]. Additionally, FoxP3 downregulation in HIV-infected Tregs was associated with lower demethylation in the *foxp3* locus [13].

Several Treg subsets with high immunosuppressive functions have been identified, including cytotoxic T lymphocyte antigen 4 $(CTLA4)^+$ Tregs, programmed cell death protein 1 $(PD1)^+$ Tregs, $CD39^+$ Tregs, and TGF-$\beta1^+$ Tregs. It has been shown that CTLA4 impedes CD28 co-stimulation by competitive binding to CD80/CD86 [1,14], and Treg-specific CTLA4 deficiency impairs Treg suppressive function [15]. $CTLA4^+$ Tregs increase during HIV infection [9,16,17] and remains higher despite antiretroviral therapy (ART) [18]. PD1 is expressed on Tregs under resting and activated conditions [19,20] and prevents the proliferation and immune responses of effector T-cells [21,22]. Untreated HIV infection increases $PD1^+$ Tregs, and their levels positively correlate with viral load and exhaustion of total CD4 and CD8 T-cells [23]. The ectonucleotidase CD39 hydrolyzes inflammatory ATP into ADP and AMP, followed by immunosuppressive adenosine production by another ectonucleotidase, CD73 [2,24,25]. Our team and others reported that $CD39^+$ Tregs and adenosine pathways are involved in suboptimal anti-HIV immune responses and disease progression, and their levels remain higher than uninfected individuals even under suppressive ART [26-28].

Another major contribution of Tregs in HIV disease progression, which starts early after HIV infection, is via TGF-β1 production, which promotes collagen-1 deposition and lymphoid tissue fibrosis [29,30]. TGF-β1 inhibits effector T-cell proliferation, suppresses the effector functions of CD8 T-cells, and promotes the differentiation of pTregs [31-33]. Tissue fibrosis is an irreversible phenomenon that obstructs cell-cell interactions and limits trafficking and homing of CD4 T-cells and IL-7 bioavailability, causing persistent immune dysregulation [29,30,34-37]. Furthermore, gut mucosal fibrosis contributes to gut dysbiosis and progressive microbial translocation from the gut to the periphery, which promotes systemic chronic inflammation and accelerated comorbidities and non-AIDS malignancies [38,39]. Notably, gut mucosal fibrosis occurs even in HIV elite controllers (EC) while they exhibit similar peripheral Treg levels compared to healthy individuals [40,41].

The acute phase of HIV infection is characterized by a rapid CD4 T-cell depletion and increased immune activation and dysfunction, mainly in the major sites of HIV replication and fibrosis, such as the gut-associated lymphoid tissues (GALT) [2,34,42-45]. Currently, it is highly recommended to initiate ART as early as possible upon HIV exposure since it improves CD4 T-cell count recovery and anti-HIV effector immune responses, while early ART decreases immune activation and viral reservoir size [43,46]. Long-term ART has been shown to decrease Treg frequency in the blood at levels similar to those of uninfected individuals [10,47]. Nevertheless, even early ART initiation was unable to completely reverse HIV-induced damaged in GALT [41,48]. However, to date, the dynamics of Treg subsets and the epigenetics status of *foxp3* gene during acute HIV infection and the impact of early ART initiation remains understudied. In this study, in HIV-infected individuals with different clinical outcomes, we evaluated the dynamic of Tregs and methylation signature of *foxp3* gene overtime during HIV infection and following early ART initiation in the acute phase. We found that early ART initiation failed to control the expansion of immunosuppressive Treg subsets and their potential migration to the gut, which might contribute to immune dysfunction and tissue fibrosis in the GALT.

2. Methods

2.1. Study population

Frozen peripheral blood mononuclear cells (PBMCs) from HIV-infected and uninfected controls were obtained from the Canadian

Cohort of HIV Infected Slow Progressors, Montreal Primary HIV Infection cohort, and McGill University Health Centre. Among study participants, 26 had acute HIV infection, defined as being within <180 days (median (IQR) 90 (43-126) days) from the estimated date of HIV infection. Chronically infected patients were either untreated (n=10) with more than one year of infection or ART-treated (n=11). HIV ECs (n=18) with undetectable plasma viral load (VL) in the absence of ART, untreated immunological controllers (ICs, n=18) with VL< 5000 copies/ml and CD4 > 400 cells/mm^3, as well as 20 HIV-uninfected controls were also included. Additionally, we prospectively assessed 20 acutely infected individuals, of whom ten had initiated ART during the acute infection, while the remaining ten patients were untreated. Follow-up specimens from the longitudinal cohorts were not included in our cross-sectional analysis.

2.2. Ethical considerations

This study was conducted according to the Declaration of Helsinki and received approval from the Ethical Review Board (#2014-452) of the Université du Québec à Montréal (UQAM). All study subjects provided written informed consent prior to their blood collection.

2.3. Flow cytometry analysis

Multiparameter flow cytometry was performed on thawed PBMCs. Optimal concentrations of fluorochrome-conjugated antibodies were used for immunological staining as detailed in **Supplementary Table 1**. Dead cells were excluded for the analysis using the LIVE/DEAD Fixable Aqua Dead Cell Stain Kit (Invitrogen, Oregon, USA). Following extracellular staining, intracellular staining of FoxP3, CTLA4, and Helios was performed after permeabilization with the Transcription Factor Buffer Set (BD Bioscience, New Jersey, USA). Data acquisition was performed on a BD LSR Fortessa X-20 cytometer, and results were analysed by FlowJo V10.7.1 (Oregon, USA).

2.4. Bisulfite DNA conversion and Nested-Polymerase chain reaction

FoxP3$^+$ CD4 T-cells were FACS-sorted using a FACs Aria III sorter (BD Biosciences) following the gating strategy presented in **Supplementary Fig. 1**. Of note, to evaluate the epigenetics status of the *foxp3* gene, only male donors were used to avoid random X chromosome inactivation in females [49]. Genomic DNA from sorted FoxP3$^+$ CD4 T-cells was isolated using the DNeasy kit (Qiagen, Hilden, Germany). Bisulfite conversion of DNA samples was conducted using the EpiTect Bisulfite Kit (Qiagen, Hilden, Germany). Six specific CpG-rich regions [50], including enhancer, proximal promoter, and CNS0-CNS3, were amplified by PCR using primers targeting specifically bisulfite converted DNA, none of which binds to areas containing CpG sites to avoid potential bias **(Supplementary Table 2)**. Briefly, PCRs were carried out in 25 μl reaction volumes containing a final concentration of 1X PCR buffer (Platinum Taq DNA polymerase, Invitrogen), 1.5 mM $MgCl_2$, 0.2 mM of dNTP mix, 0.4 μM forward and reverse primers, and 2-4 μl of bisulfite DNA template (external PCR) or external PCR product (internal PCR). The thermocycling program used was as follows: 95°C for 2 min, followed by 40 cycles of 95°C for 30 s, Tm for 40 s, 72°C for 1 min, and a final extension step of 72°C for 10 min. The optimized Tm for each region was as follows: 50°C for proximal promoter, 58.1°C for enhancer, 51.8°C for CNS0 and CNS3, 52.7°C for CNS1, and 59.1°C for CNS2. Following amplification, the quality of PCR products was assessed on a 2% agarose gel.

2.5. Next-generation sequencing

PCR products were purified using Just-a-plate 96 PCR purification and normalization kit (Charm Biotech, MA, USA). The libraries were then generated by pooling 5 μl of each sample, and the cleanup steps were performed using AMPure XP Beads (Beckman Coulter, California, USA). Purified libraries were quantified using the Qubit dsDNA HS assay (Life Technologies, California, USA) and the NEBNext Library Quant Kit for Illumina (New England Biolabs, MA, USA). The average size fragment was determined using a high sensitivity DNA assay on the 2100 Bioanalyzer System (Agilent, California, USA). Finally, the amplicon pool was spiked with 12% of PhiX control (loaded at a final concentration of 6 pM), and sequencing was performed using the MiSeq® Reagent Kit v3 cartridge 600 cycles (PE300) (Illumina). Library preparation and sequencing were carried out at the Genomics Core of the CERMO-FC research center, UQAM.

2.6. Bioinformatic analysis

Bisulfite treated sequences within FASTQ files were trimmed for adapters and bases of quality lower than 30 at the 3′ extremities using TrimGalore version 0.4.5. Trimmed reads were then mapped on chromosome X of the human genome GRCh37 using Bismark version 0.19.0. Default parameters were used for the alignment, which was performed with Bowtie 2.1.0. Bioinformatic analysis was done by the Bioinformatics Core Facility at the Institute for Research in Immunology and Cancer, *Université de Montréal*.

2.7. Statistical analysis

Statistical analysis was performed using GraphPad Prism V6.01 (California, USA). Results are presented throughout the text as median with interquartile range (IQR). The distribution of variables was initially determined by the Kolmogorov–Smirnov test. Then, the Kruskal–Wallis test was performed to determine whether significant differences exist between the six study groups. Nonparametric Mann-Whitney and Wilcoxon rank tests were used for unpaired and paired variables, respectively. The Spearman correlation coefficient test established the correlation between variables. Only statistical significances ($p<0.05$) are presented in the figures (*, $P < 0.05$; **, $P < 0.01$; ***, $P < 0.001$; ****, $P < 0.0001$).

2.8. Role of funding source

Funders had no role in study design, data collection, data analyses, interpretation, or writing of report.

3. Results

3.1. Characteristics of the study populations

Chronically infected individuals on ART in the cross-sectional study *versus* chronically infected individuals on ART in the longitudinal study were significantly older (median age: 51 *versus* 36.5 years, Mann-Whitney p= 0.04) with longer duration of HIV infection (median: 12.7 *versus* 2.27 years, $p<0.0001$) and on longer duration on ART (median: 14.58 *versus* 1.72 years, Mann-Whitney p=0.0002). ART initiation in these individuals was also more delayed (median years of ART initiation post-infection of 1.11 *versus* 0.46 years, Mann-Whitney p=0.05) (**Tables 1**, **2**). We thus assessed the impact of early ART on our study measures based on the longitudinal analysis. In chronic infection, ART normalized the CD4 T-cell count, yet the CD8 T-cell count remained elevated compared to uninfected individuals. Consequently, despite improved CD4/CD8 ratio, early ART was unable to normalize this parameter in treated individuals. EC and IC exhibit CD4 T-cell counts similar to uninfected individuals, despite higher

Table 1
Clinical characteristics of study groups.

Characteristics	Study population (n=103)						*p-values*
	Non-infected (n=20)	Acute (n=26)	Chronic ART- (n=10)	Chronic ART+ (n=11)	EC (n=18)	IC (n=18)	
Male sex, n (%)	15[a] (75%)	26[a,h,i] (100%)	10[k,l] (100%)	11[.m,n] (100%)	10[h,k,m] (55.6%)	10[i,l,n] (55.6%)	$p<0.0001$
Age, years [median (IQR)]	39[d] (30.75-47)	39.5[g,h] (32.75-43)	32.5[j,k] (26-39.75)	51[g,j,n] (41-60)	49[d,h,k,o] (32-55.5)	35[n,o] (31.5-40.75)	$p=0.0005$
Nadir CD4+ cell count, cells/μl [median (IQR)]	NA	330[i] (257.8-500)	310[l] (245-423.5)	334 (297.8-533.5)	551.5 (301.5-624.8)	459.5[i,l,] (399-592.5)	$p=0.07$
CD4+ T-cell count, cells/μl [median (IQR)]	632[b] (463.5-775)	460[h,i] (380-610)	440[b,k,l] (255-543)	603 (400-847)	730[h,k] (638.5-900)	680[i,l] (614-806.5)	$p=0.0002$
CD8+ T-cell count, cells/μl [median (IQR)]	197[a,b,c,d,e] (153-428.5)	996[a] (640-1630)	750[b] (629-1133)	743[c] (433.3-1192)	739[d] (604-1040)	808[e] (478.8-1213)	$p=0.0003$
CD4+/CD8+ T-cell count ratio [median (IQR)]	2.82[a,b,c,d,e] (1.41-4.19)	0.46[a,g,h,i] (0.21-1.14)	0.48[b,j,k,l] (0.40-0.61)	0.87[c,g,j] (0.60-1.81)	0.95[d,h,k,n] (0.80-1.43)	0.81[e,i,l,n] (0.55-1.42)	$p<0.0001$
Viral load, $\log_{10}$ copies/mL [median (IQR)]	NA	4.36[g,h,i] (3.82-5.50)	4.56[j,k,l] (3.74-3.98)	1.60[g,j,n] (1.60-1.60)	1.65[h,k,o] (1.60-1.69)	2.91[i,l,n,o] (2.57-3.34)	$p<0.0001$
Duration of infection, years [median (IQR)]	NA	0.25[f,g,h,i] (0.12-0.35)	2.55[f,j,k,l] (1.54-4.26)	12.40[g,j] (4.99-19.33)	15.3[h,k,o] (7.87-21)	7.55[i,l,o] (2.9-11.08)	$p<0.0001$
Time of ART initiation years post-infection [median (IQR)]	NA	NA	NA	1.11 (0.49-2.02)	NA	NA	NA
Duration of ART, years [median (IQR)]	NA	NA	NA	14.58 (3.56-20.73)	NA	NA	NA

Results are shown as median and interquartile range (IQR).
NA: not applicable, EC: Elite controllers, IC: Immunological controllers
p-values come from comparing the six groups using the Kruskal-Wallis test. Significant differences ($p < 0.05$) following Mann−Whitney U test or Fisher's test are mentioned as follow:
a: Non-infected vs Acute, b: Non-infected vs Chronic (ART-), c: Non infected vs Chronic (ART+), d: Non-infected vs EC, e: Non-infected vs IC, f: Acute vs Chronic (ART-), g: Acute vs Chronic (ART+), h: Acute vs EC, i: Acute vs IC, j: Chronic (ART-) vs Chronic (ART+), k: Chronic (ART-) vs EC, l: Chronic (ART-) vs IC, m: Chronic (ART+) vs EC, n: Chronic (ART+) vs IC, o: EC vs IC

CD8 T-cell counts. Besides, individuals with chronic infection on long-term ART and ECs groups were the oldest study group with the longest duration of HIV infection. In longitudinal specimens, after early ART initiation, the CD4 T-cell count and CD4/CD8 ratio were improved significantly (Wilcoxon p=0.04 and p=0.002, respectively). Of note, no significant difference was detected between clinical characteristics of two n=10 acute individuals in untreated and treated longitudinal sub-groups (**Table 2**). All ART-treated individuals had a plasma VL below the level of detection. The clinical characteristics of study participants are described in Tables 1 and 2.

3.2. Early ART initiation decreased but did not normalize T-cell immune activation and senescence

As expected, untreated HIV infection was associated with increased $CD38^{+}HLADR^{+}$ activated CD4 and CD8 T-cells (**Fig. 1a, d, e**).

Table 2
Clinical characteristics of longitudinal samples.

Characteristics	Longitudinal specimens			
	Untreated		ART-Treated	
	Acute (n=10)	Chronic ART- (n=10)	Acute (n=10)	Chronic ART+ (n=10)
Male sex, n (%)	10 (100%)	10 (100%)	10 (100%)	10 (100%)
Age, years [median (IQR)]	39.5 (35.50-43.25)	39.5 (34.75-43)	36 (29.75-46.50)	36.5 (29-46.5)
Nadir CD4+ cell count, cells/μl [median (rangeIQR)]	365 (297.5-525)	NA	258.5 (207.5-530)	NA
CD4+ T-cell count, cells/μl [median (IQR)]	515 (419-767.5)	595 (287.5-813.8)	450[b] (272.5-561.3)	521[b] (377.5-795)
CD8+ T-cell count, cells/μl [median (IQR)]	830[a] (615-1170)	953[a] (705-1915)	1019 (580-1708)	655 (531-1081)
CD4+/CD8+ T-cell count ratio [median (IQR)]	0.56[a] (0.40-1.35)	0.50[a] (0.32-0.85)	0.40[b] (0.19-0.81)	0.69[b] (0.40-1.24)
Viral load, $\log_{10}$ copies/mL [median (IQR)]	4.07[a] (3.54-4.37)	4.60[a] (4.01-5.20)	4.40[b] (3.92-5.77)	1.70[b] (1.67-1.70)
Duration of infection, years [median (IQR)]	0.22[a] (0.11-0.36)	2.19[a] (2.12-2.39)	0.28[b] (0.13-0.39)	2.27[b] (2.00-2.646)
Time of ART initiation years post-infection, years [median (IQR)]	NA	NA	NA	0.46 (0.27-0.59)
Duration of ART, years [median (IQR)]	NA	NA	NA	1.72 (1.43-1.99)

Results are shown as median and interquartile range (IQR).
NA: not applicable
Significant differences ($p < 0.05$) following Wilcoxon signed-rank test are mentioned as follow:
a: Acute vs Chronic (ART-), b: Acute vs Chronic (ART+)

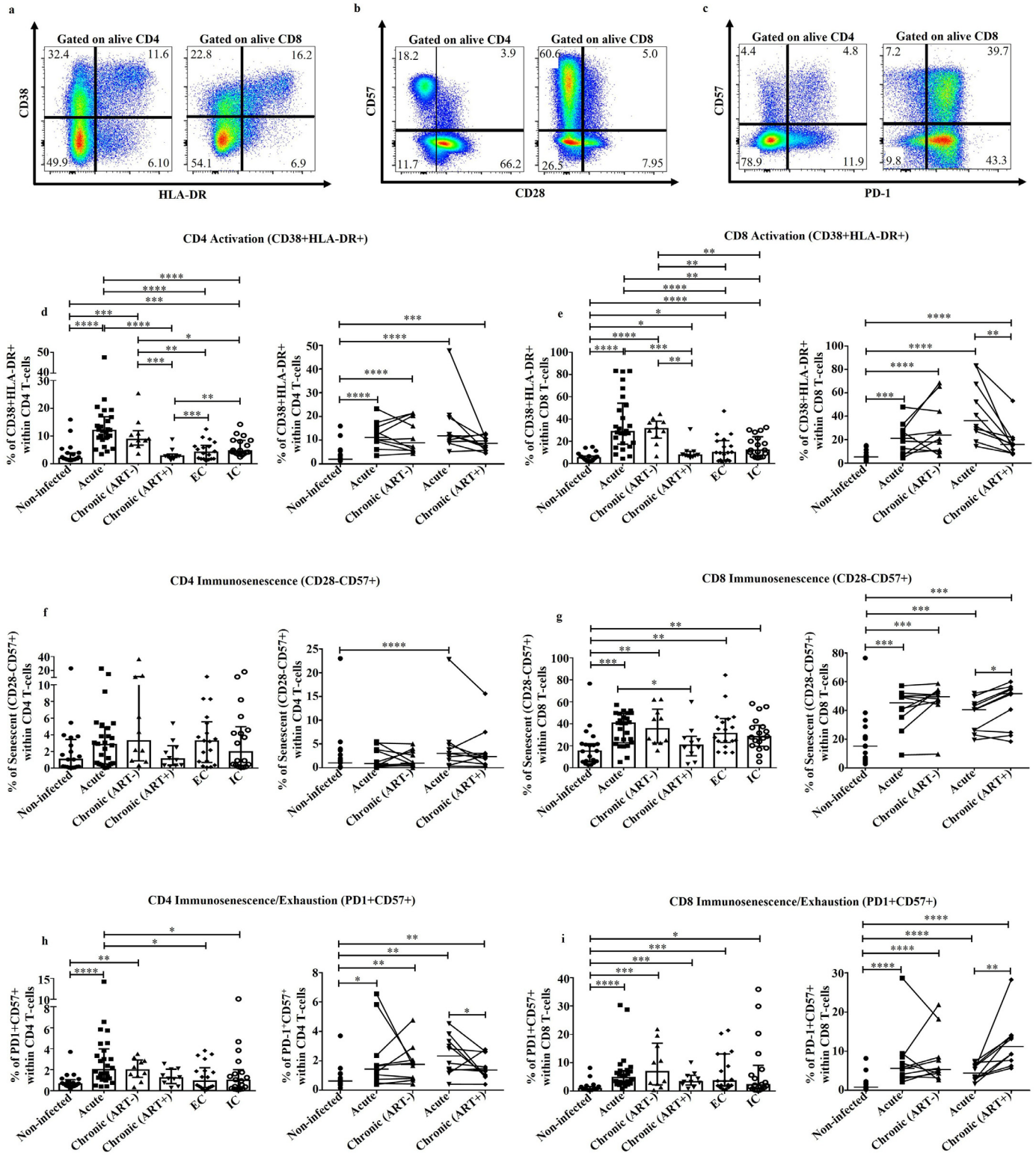

Figure 1. Levels of CD4 and CD8 T-cell immune-activation, immunosenescence and exhaustion among study groups. Gating strategies used to define (**a**) activated (HLA-DR$^+$CD38$^+$) CD4 and CD8 T-cells, (**b**) immunosenescence (CD28$^-$CD57$^+$) CD4 and CD8 T-cells, and (**c**) exhausted (PD1$^+$CD57$^+$) CD4 and CD8 T-cells. Percentages of immune-activated (HLA-DR$^+$CD38$^+$) CD4 (**d**) and CD8 T-cells (**e**). Percentages of immunosenescent (CD28$^-$CD57$^+$) CD4 (**f**) and CD8 T-cells (**g**). Percentages of exhausted (PD1$^+$CD57$^+$) CD4 (**h**) and CD8 T-cells (**i**). Statistical significance is indicated in the figures (*, $P < 0.05$; **, $P < 0.01$; ***, $P < 0.001$; ****, $P < 0.0001$). Differences among six study groups was determined by nonparametric Mann-Whitney rank test for unpaired variables, while the Wilcoxon rank tests were used for paired variables in the follow-up study. Sample size in Cross-sectional analysis: non-infected n=20, Acute n=26, Chronic ART- n=10, Chronic ART+ n=11, EC n=18, IC n=18; Sample size in longitudinal analysis: non-infected n=20, ART- n=10, ART+ n=10.

Early ART initiation reduced CD8 T-cell immune activation (Wilcoxon p=0.002), while their levels remained higher than those of HIV-uninfected controls (Mann-Whitney p<0.0001; Fig 1**d, e**). HIV infection increased the frequencies of both senescent (CD28$^-$CD57$^+$) and exhausted (PD1$^+$CD57$^+$) CD8 T-cells in all study groups (Fig. 1**b, g, i**), while early ART initiation failed to mitigate this increase (Mann-

Whitney p=0.0004 and p<0.0001, respectively). HIV infection also increased levels of CD4 T-cell exhaustion, which was reduced but not normalized by early ART (Mann-Whitney p=0.009; **Fig. 1c, h**), while no difference in senescent CD4 T-cells was observed among study groups (**Fig. 1b, f**). Both CD4 and CD8 T-cell immune activation and senescence correlated negatively with CD4/CD8 ratios and positively with VL (**Supplementary Fig. 2**). Interestingly, significant decreases in CD4 and CD8 immune activation, and CD8 exhaustion, were correlated with the duration of ART (**Table 3**). EC and IC groups presented significantly lower CD4 and CD8 immune activation than untreated HIV-infected individuals, while their CD8 immune activation, senescence, and exhaustion remained higher than uninfected controls (**Fig. 1**).

3.3. Early ART initiation suppressed the expansion of total Tregs

Chronic HIV infection was associated with an increase in total Treg ($CD4^+CD25^{high}CD127^{low}FoxP3^+$) frequencies compared to uninfected individuals (Mann-Whitney p<0.01 in both cross-sectional and longitudinal analysis), which was suppressed following early ART initiation (**Fig 2a, b**). The frequency of total Tregs was inversely correlated with CD4/CD8 ratio and positively with CD4 immune activation (**Supplementary Fig. 3**). Treg frequencies in ECs and ICs were lower than chronically untreated HIV+ individuals (Mann-Whitney p<0.05 for both comparisons) and similar to uninfected individuals (**Fig 2b**). We also found heterogeneity in Treg differentiation in HIV-infected individuals compared to uninfected controls (**Fig. 2a, c-f**). Indeed, acute HIV infection was associated with an increase in the frequencies of naïve Tregs (Mann-Whitney p=0.001), along with a decrease in central memory (CM, Mann-Whitney p=0.003) and effector memory (EM, Mann-Whitney p<0.0001) Tregs (**Fig. 2c-e**). In longitudinal analysis, early ART initiation didn't affect these subsets. However, longer duration of ART was associated with significant increases CM and EM Tregs (Spearman p=0.007 and p=0.02, respectively) and with a decline in naïve and TD Tregs (Spearman p<0.0001 and p=0.03, respectively; **Table 3**). Interestingly, the EC group had similar frequencies of naïve, CM and EM and lower terminally differentiated (TD) Tregs compared to uninfected individuals (**Fig. 2c, f**). These results collectively showed that early ART initiation controlled the expansion of Tregs and affected the distribution of their memory subsets.

Table 3
Correlation between clinical and immunological parameters and duration of ART (years).

Correlations with duration of ART (years)		
Immunological measure	r	*p*-value
CD4 T-cells count	0.1030	0.7
CD8 T-cells count	0.0088	0.9
CD4/CD8 ratio	0.0558	0.8
CD4 Activation ($CD4^+HLA\text{-}DR^+CD38^+$)	-0.5563	**0.02**
CD4 Immunosenescence ($CD4^+CD57^+CD28^-$)	-0.2735	0.3
CD4 exhaustion ($CD4^+CD57^+PD1^+$)	-0.3076	0.2
CD8 activation ($CD8^+HLA\text{-}DR^+CD38^+$)	-0.6176	**0.01**
CD8 Immunosenescence ($CD8^+CD57^+CD28^-$)	-0.2176	0.4
CD8 exhaustion ($CD8^+CD57^+PD1^+$)	-0.6176	**0.01**
Total Tregs ($CD4^+CD25^{high}CD127^{low}FoxP3^+$)	-0.4495	0.07
Naïve Tregs ($CD45RA^+CD28^+$ Tregs)	-0.8374	< **0.0001**
CM Tregs ($CD45RA^-CD28^+$ Tregs)	0.6559	**0.007**
EM Tregs ($CD45RA^-CD28^-$ Tregs)	0.5567	**0.02**
TD Tregs ($CD45RA^+CD28^-$ Tregs)	-0.5243	**0.03**
$CTLA4^+$ Tregs	-0.0911	0.7
$PD1^+$ Tregs	-0.5765	**0.02**
$CTLA4^+PD1^+$ Tregs	-0.3429	0.1
Mem $CTLA4^+PD1^-FoxP3^+$	0.0235	0.9
$CD39^+$ Tregs	0.07506	0.7
LAP(TGF-β1)$^+$ Tregs	-0.5085	**0.04**
CD39+LAP(TGF-β1)$^+$ Tregs	-0.1927	0.4
$CXCR3^+$ Tregs	-0.5901	**0.01**
$CCR6^+$ Tregs	-0.7334	**0.001**
Integrin $\beta7^+$ Tregs	-0.6500	**0.007**
$CCR9^+$ Tregs	-0.5321	**0.03**
Integrin $\beta7^+CD39^+$ Tregs	-0.5063	**0.04**
Integrin $\beta7^+$LAP(TGF-β1)$^+$ Tregs	-0.5950	**0.01**
$CCR9^+CD39^+$ Tregs	-0.3812	0.1
$CCR9^+$LAP(TGF-β1)$^+$ Tregs	-0.4183	0.1
Th17 cells	-0.3765	0.15
Th17/Treg ratio	-0.3029	0.25
$CD31^-FoxP3^+$	-0.5441	**0.03**
$CD31^+FoxP3^+$	-0.6696	**0.005**
$Helios^-FoxP3^+$	-0.6265	**0.01**
$Helios^+FoxP3^+$	-0.4059	0.12
$HLA\text{-}DR^+CD38^+FoxP3^+$	-0.5578	**0.02**
CNS1 demethylation	-0.1655	0.5

p-values come from the comparison of clinical and immunological parameters with the duration of ART (years) by using the Spearman correlation coefficient test.
Significant differences (p < 0.05) are highlighted in Bold.

3.4. Early ART initiation failed to normalize Treg subsets known for their highly immunosuppressive capacity

As mentioned before, various Tregs subsets, including $CTLA4^+$ [9,16,17], $PD1^+$ [23], $CD39^+$ [26-28], and TGF-$\beta1^+$ [29] Tregs increase during untreated HIV infection and impact negatively in the outcome of the disease. Herein, we observed an increase in the frequencies of $CTLA4^+$ Tregs, $PD1^+$ Tregs, and $CTLA4^+PD1^+$ Tregs (Mann-Whitney p=0.005, p<0.0001 and p<0.0001, respectively) during acute HIV infection compared to uninfected individuals, which were not restored longitudinally after early ART initiation (**Fig. 3a, d-f**). Meanwhile, longer duration of ART was associated with a decline in PD1-expressing Tregs (Spearman p=0.02; **Fig 3e, f; Table 3**). ECs and ICs showed lower $CTLA4^+$ Tregs, $PD1^+$ Tregs, and $CTLA4^+PD1^+$ Tregs frequencies than acute HIV-infected group while similar $CTLA4^+$ Tregs and $CTLA4^+PD1^+$ Treg than uninfected controls (**Fig. 3d-f**). A new subset of memory CD4 T-cells that share Treg characteristics described as memory $CTLA4^+PD1^-FoxP3^+$ has been recently proposed as viral reservoirs within peripheral lymph nodes of ART-treated SIV-infected rhesus macaques [51]. In this regard, we found that acute HIV infection increased the frequencies of these cells compared to uninfected individuals (p=0.04), while early ART could not restore their frequencies, suggesting a potential contribution of Tregs in viral persistence despite early ART (**Fig. 3b, g**).

Higher $CD39^+$ Tregs were observed in acute HIV-infected and ART-treated individuals compared to uninfected controls (Mann-Whitney p=0.02 and p<0.0001, respectively), and ART duration didn't affect $CD39^+$ Tregs frequencies (**Fig. 3c, h; Table 3**). In concordance with a previous report [16], EC had similar $CD39^+$ Treg frequencies than uninfected controls (**Fig. 3h**). TGF-β1 is initially synthesized as a pro-TGF-β1, which is further cleaved to produce the dimeric propeptides called a latency-associated peptide (LAP) that associates non-covalently with mature TGF-β to prevent TGF-β1 binding to its receptor and subsequent activity [52]. LAP(TGF-β1)$^+$ Tregs and $CD39^+$LAP(TGF-β1)$^+$ Tregs populations (**Fig. 3c, i, j**) were increased during HIV infection *versus* uninfected individuals (Mann-Whitney p<0.0001 for both comparison) and were not reduced upon early ART initiation. Interestingly, the frequencies of LAP(TGF-β1)$^+$ Tregs correlated negatively with duration of ART (Spearman p=0.04; **Table 3**) and CD4/CD8 ratio (Spearman p=0.002) and positively with immune activation (Spearman p=0.04 for CD4 and p=0.01 for CD8 activation; **Supplementary Fig. 4**). In addition, the frequencies of LAP(TGF-β1)$^+$ Tregs remained elevated in EC group compared to uninfected controls (Mann-Whitney p=0.01). Overall, our data demonstrated that early ART initiation was unable to normalize the frequencies of immunosuppressive Treg subsets, nor did it affect the frequencies of a Treg population previously described as a viral reservoir (Memory $CTLA4^+PD1^-FoxP3^+$ T-cells).

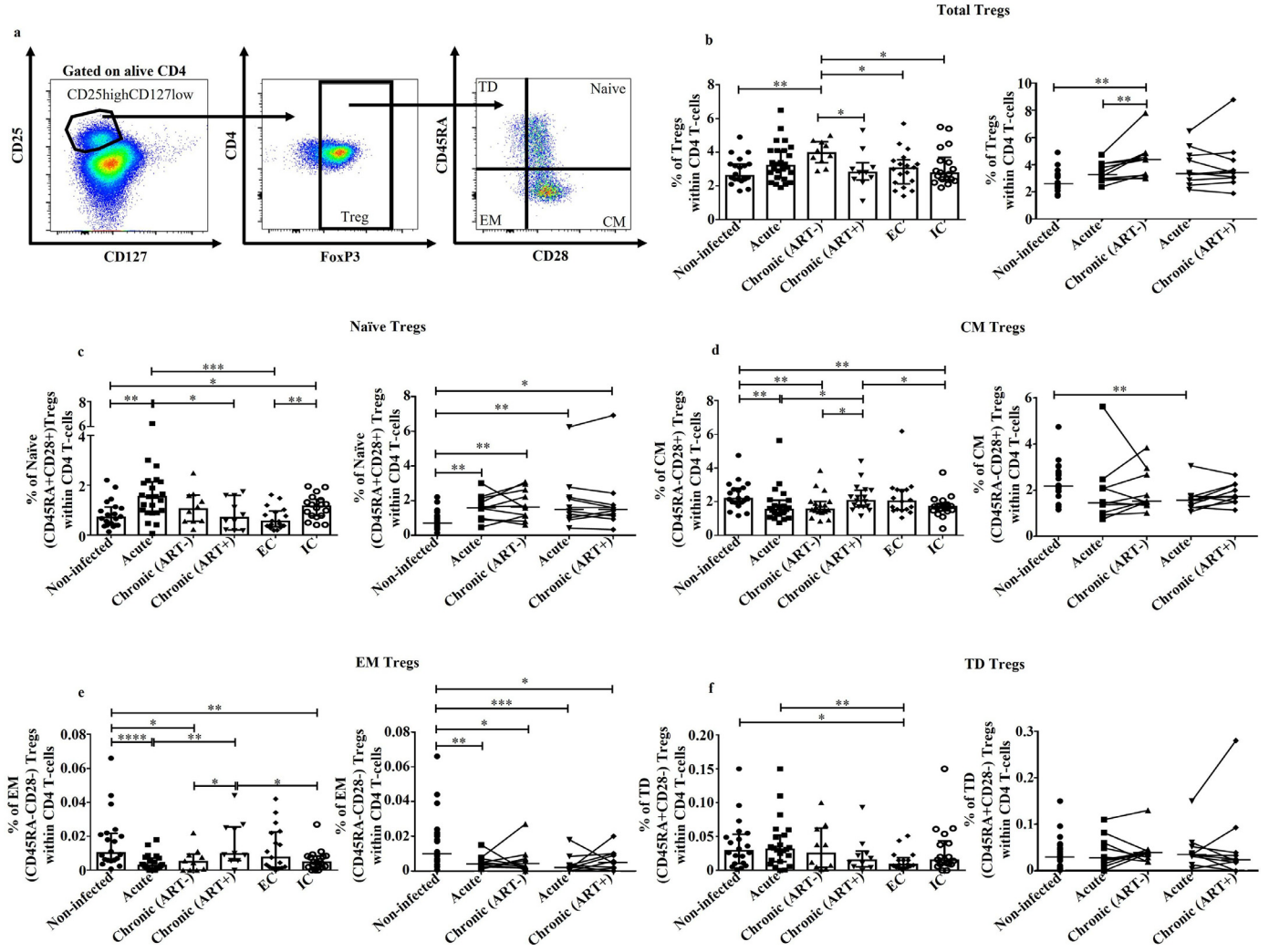

Figure 2. Changes in the frequencies of total Tregs and Treg memory subsets among study groups. (**a**) Gating strategies used to define total Tregs ($CD4^+CD25^{high}CD127^{low}FoxP3^+$) and Tregs subsets within CD4 T-cells. (**b**) Percentages of total Treg. Frequencies of (**c**) naïve ($CD45RA^+CD28^+$), (**d**) central memory (CM, $CD45RA^-CD28^+$), (**e**) effector memory (EM, $CD45RA^-CD28^-$) and (**f**) terminally differentiated (TD, $CD45RA^+CD28^-$) Treg subsets. Statistical significance is indicated in the figures (*, $P < 0.05$; **, $P < 0.01$; ***, $P < 0.001$; ****, $P < 0.0001$). Differences among six study groups was determined by nonparametric Mann-Whitney rank test for unpaired variables, while the Wilcoxon rank tests were used for paired variables in the follow-up study. Sample size in Cross-sectional analysis: non-infected n=20, Acute n=26, Chronic ART- n=10, Chronic ART+ n=11, EC n=18, IC n=18; Sample size in longitudinal analysis: non-infected n=20, ART- n=10, ART+ n=10.

3.5. Early ART failed to normalize Tregs migration potential toward the gut

We previously demonstrated that Treg accumulation within GALT begins in acute HIV infection [28]. To assess the Treg capacity to migrate to inflammatory tissues and the gut, we analysed the expression of CXCR3 [53,54] and CCR6 [55] which mediate Treg recruitment to mucosal and inflammatory sites. HIV infection increased both $CXCR3^+$ and $CCR6^+$ Treg subsets, while early ART initiation was unable to normalize the $CCR6^+$ Tregs levels (**Fig. 4a, g, h**). Furthermore, we also assessed the expression of Integrin-$\beta7^+$, which directs Tregs migration from blood into the gut via the interaction with Mucosal vascular-Addressin Cell-Adhesin Molecule 1 [56-60] and CCR9, a chemokine receptor that binds to CCL25 and promotes Treg migration to the small intestine [60-62]. HIV infection was associated with an increase in Integrin-$\beta7^+$ and $CCR9^+$ Tregs starting in the acute phase, which were not restored by early ART initiation (**Fig 4b, i, j**). Notably, $CD39^+$ and LAP(TGF-$\beta1$)$^+$ Tregs with gut migratory potential such as Integrin-$\beta7^+CD39^+$, Integrin-$\beta7^+$LAP(TGF-$\beta1$)$^+$, $CCR9^+CD39^+$ and $CCR9^+$LAP(TGF-$\beta1$)$^+$ (Mann-Whitney p=0.0004, p=<0.0001, p=0.0017, p=0.0019; respectively) Tregs were all increased during acute HIV infection compared to uninfected participants and were not restored following early ART initiation (**Fig. 4c-f, k-n**). However, a significant decline was observed in frequencies of Tregs expressing gut homing markers along with the longer duration of ART (**Table 3**). Significantly, the frequencies of $CCR9^+CD39^+$, $CCR9^+$LAP(TGF-$\beta1$)$^+$, Integrin-$\beta7^+CD39^+$, and Integrin-$\beta7^+$LAP(TGF-$\beta1$)$^+$ Tregs positively correlated with CD4 and CD8 immune activation, and negatively with CD4/CD8 ratio as an indicator of disease progression (**Supplementary Fig. 5**). A positive correlation was observed between VL and $CCR9^+$LAP(TGF-$\beta1$)$^+$ and Integrin $\beta7^+$LAP(TGF-$\beta1$)$^+$ Tregs, while no correlation was detected with $CCR9^+CD39^+$ and Integrin $\beta7^+CD39^+$ Tregs (**Supplementary Fig. 5**), suggesting the accumulation of $CD39^+$ Tregs in the gut regardless of VL.

ECs and ICs represented similar levels of $CXCR3^+$, Integrin $\beta7^+$, $CCR9^+$, Integrin $\beta7^+CD39^+$ and $CCR9^+CD39^+$ Tregs than uninfected individuals. Importantly, Integrin-$\beta7^+$LAP(TGF-$\beta1$)$^+$ Tregs and $CCR9^+$LAP(TGF-$\beta1$)$^+$ Tregs were significantly higher in ECs (Mann-Whitney p=0.03 and p=0.004, respectively) and ICs (Mann-Whitney p=0.005 and p=0.003, respectively) than uninfected individuals, suggesting the accumulation of pro-fibrotic Tregs even in these individuals (**Fig 4**). Moreover, lower frequencies of $CCR6^+$ Tregs were observed in EC individuals compared to HIV uninfected controls

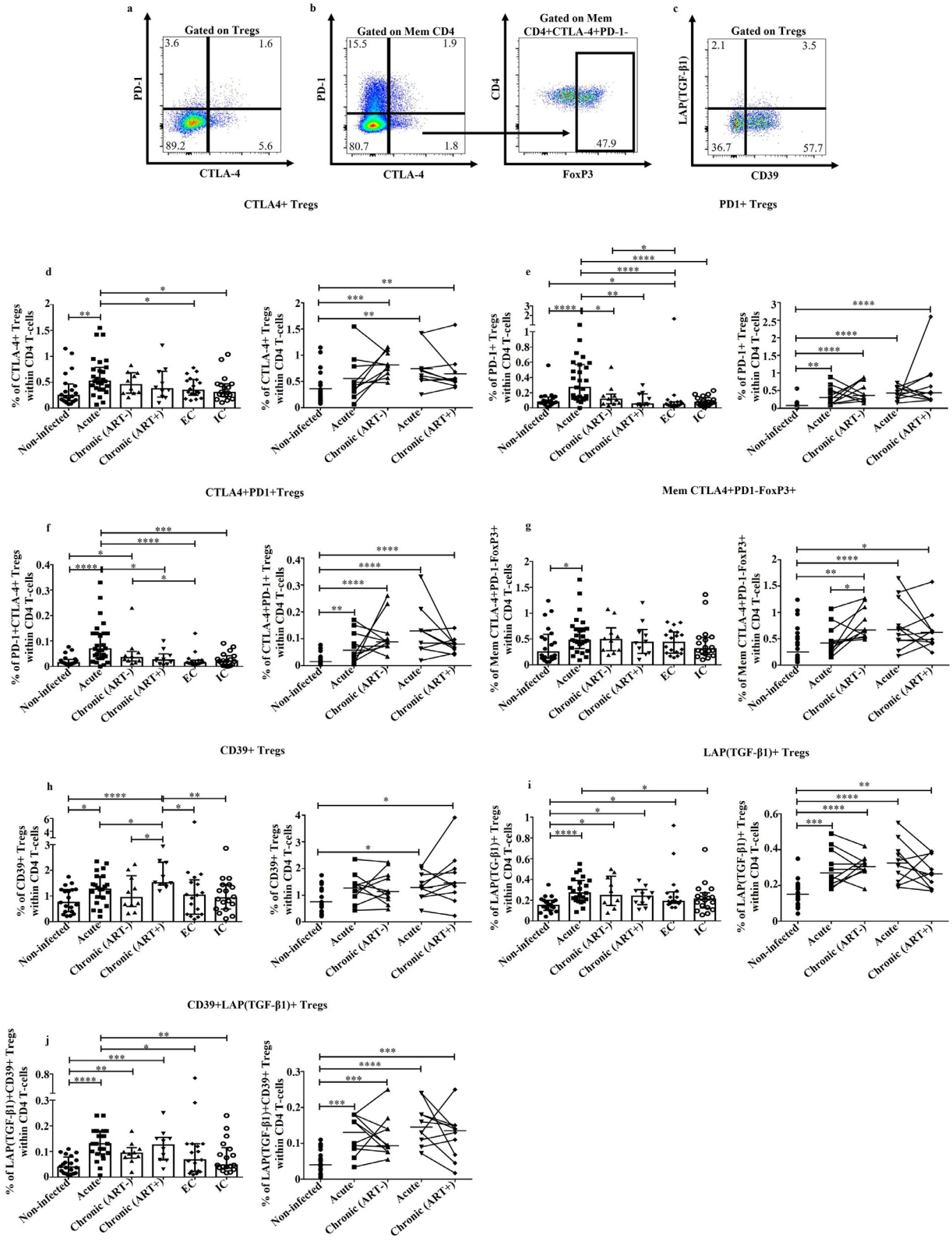

Figure 3. Early ART initiation was unable to normalize Tregs subsets with known immunosuppressive functions. Gating strategies used to define (**a**) CTLA4$^+$ and PD1$^+$ Tregs, (**b**) Memory (CD45RA$^-$) CTLA4$^+$PD1$^-$FoxP3$^+$ CD4 T-cells, (**c**) CD39$^+$ and LAP(TGF-β1)$^+$ Tregs. d)Percentages of CTLA4$^+$ Tregs within CD4 T-cells. (**e**) Percentages of PD1$^+$ Tregs within CD4 T-cells. **f**) Percentages of CTLA4$^+$PD1$^+$ Tregs within CD4 T-cells. (**g**) Percentages of Memory CTLA4$^+$PD1$^-$FoxP3$^+$ within CD4 T-cells. **h**) Percentages of CD39$^+$ Tregs within CD4 T-cells. **i**) Percentages of LAP(TGF-β1)$^+$ Tregs within CD4 T-cells. **j**) Percentages of CD39$^+$LAP(TGF-β1)$^+$ Tregs within CD4 T-cells. Statistical significance is indicated in the figures (*, $P < 0.05$; **, $P < 0.01$; ***, $P < 0.001$; ****, $P < 0.0001$). Differences among six study groups was determined by nonparametric Mann-Whitney rank test for unpaired variables, while the Wilcoxon rank tests were used for paired variables in the follow-up study. Sample size in Cross-sectional analysis: non-infected n=20, Acute n=26, Chronic ART- n=10, Chronic ART+ n=11, EC n=18, IC n=18; Sample size in longitudinal analysis: non-infected n=20, ART- n=10, ART+ n=10.

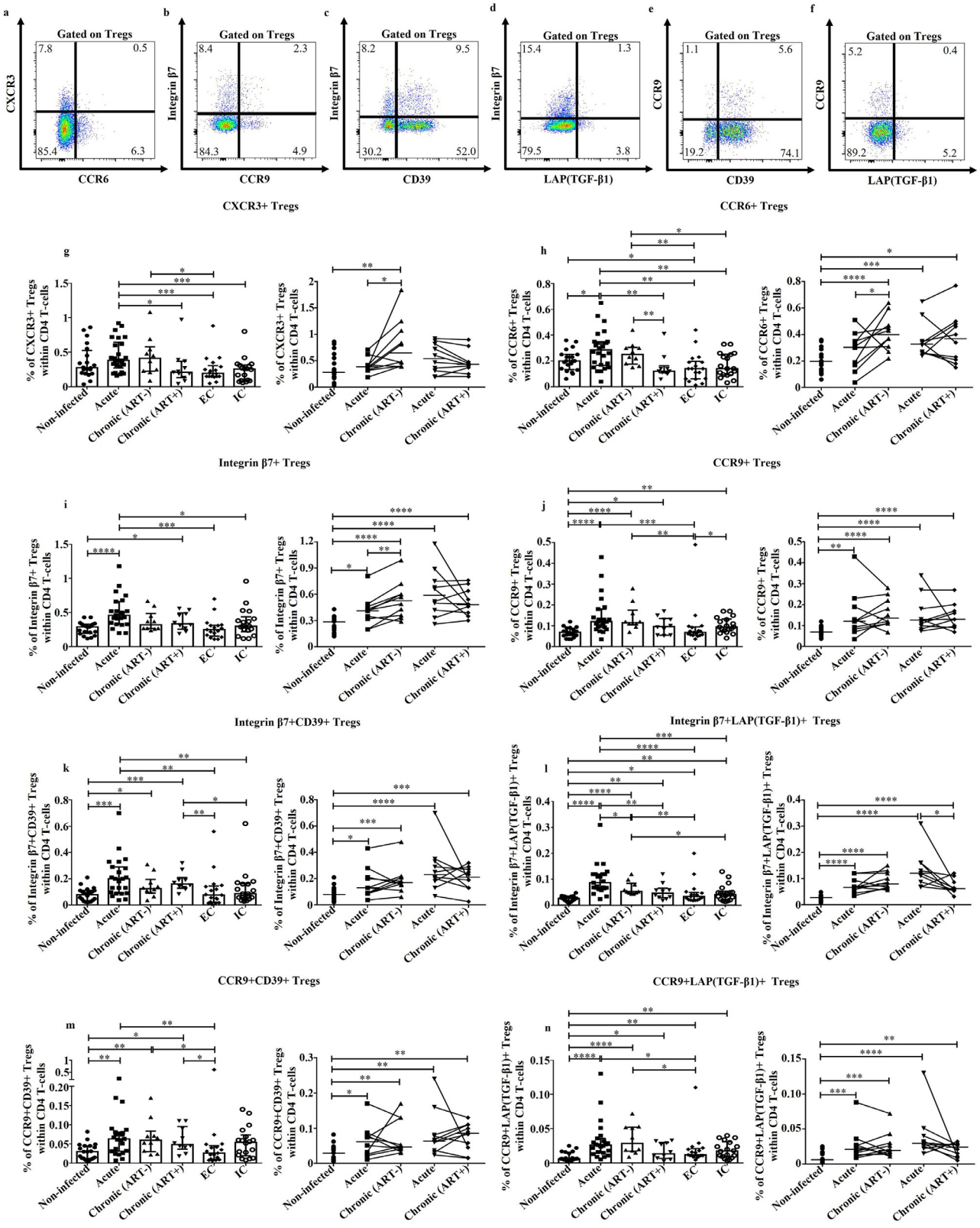

Figure 4. Impact of early ART initiation on Tregs migratory potential toward the gut. Gating strategies used to define (**a**) CXCR3$^+$ and CCR6$^+$ Tregs, (**b**) CCR9$^+$ and Integrin-$\beta7^+$ Tregs, (**c**) Integrin-$\beta7^+$CD39$^+$ Tregs, (**d**) Integrin-$\beta7^+$LAP(TGF-$\beta1$)$^+$ Tregs, (**e**) CCR9$^+$CD39$^+$ Tregs, (**f**) CCR9$^+$LAP(TGF-$\beta1$)$^+$ Tregs. (**g**) Percentages of CXCR3$^+$ Tregs within CD4 T-cells. (**h**) Percentages of CCR6$^+$ Tregs within CD4 T-cells. (**i**) Percentages of Integrin-$\beta7^+$ Tregs within CD4 T-cells. (**j**) Percentages of CCR9$^+$ Tregs within CD4 T-cells. (**k**) Percentages of Integrin-$\beta7^+$CD39$^+$ Tregs within CD4 T-cells. (**l**) Percentages of Integrin-$\beta7^+$LAP(TGF-$\beta1$)$^+$ Tregs within CD4 T-cells. (**m**) Percentages of CCR9$^+$CD39$^+$ Tregs within CD4 T-cells. **n**) Percentages of CCR9$^+$LAP(TGF-$\beta1$)$^+$ Tregs within CD4 T-cells. Statistical significance is indicated in the figures (*, $P < 0.05$; **, $P < 0.01$; ***, $P < 0.001$; ****, $P < 0.0001$). Differences among six study groups was determined by nonparametric Mann-Whitney rank test for unpaired variables, while the Wilcoxon rank tests were used for paired variables in the follow-up study. Sample size in Cross-sectional analysis: non-infected n=20, Acute n=26, Chronic ART- n=10, Chronic ART+ n=11, EC n=18, IC n=18; Sample size in longitudinal analysis: non-infected n=20, ART- n=10, ART+ n=10.

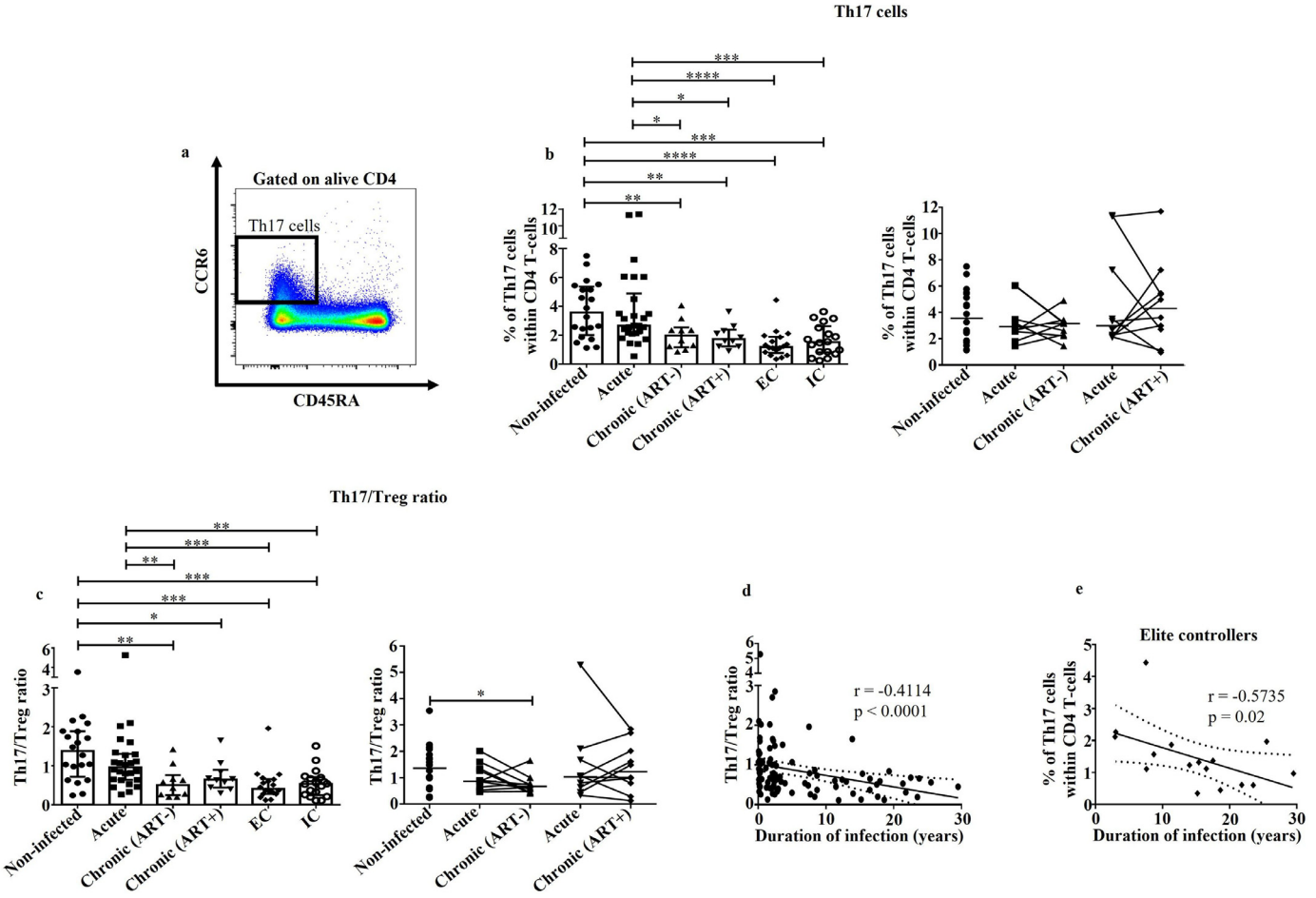

Figure 5. Frequencies of Th17 cells and Th17/Treg ratio overtime during HIV infection and following early ART. (**a**) Gating strategy used to define Th17 cells ($CD4^+CD45RA^-CCR6^+$). (**b**) Percentages of Th17 cells within CD4 T-cells. (**c**) Th17/Treg ratio. (**d**) Correlation between duration of the infection (years) and Th17/Treg ratio within all study groups. (**e**) Correlation between duration of the infection (years) and Th17 cells frequencies within elite controllers. Statistical significance is indicated in the figures (*, $P < 0.05$; **, $P < 0.01$; ***, $P < 0.001$; ****, $P < 0.0001$). Differences among six study groups was determined by nonparametric Mann-Whitney rank test for unpaired variables, while the Wilcoxon rank tests were used for paired variables in the follow-up study. Sample size in Cross-sectional analysis: non-infected n=20, Acute n=26, Chronic ART- n=10, Chronic ART+ n=11, EC n=18, IC n=18; Sample size in longitudinal analysis: non-infected n=20, ART- n=10, ART+ n=10.

(Fig. 4**h**). Altogether, our results showed that, during HIV infection and despite early ART initiation, immunosuppressive $CD39^+$ and LAP $(TGF\text{-}\beta1)^+$ Tregs continued to migrate to the gut which, in turn, could contribute to disease progression and mucosal fibrosis.

3.6. Early ART initiation restored Th17/Treg ratio

Memory $CCR6^+$ Th17 cells are highly permissive to HIV infection and are rapidly depleted following the infection, which results in the breakdown of gut mucosal integrity and microbial translocation [42,63,64]. Here, the frequency of Th17 cells was lower among both untreated and ART^+ chronically infected individuals compared to uninfected controls (Mann-Whitney p=0.0093 and p=0.0099, respectively), while early ART was unable to affect their frequencies (Fig. 5**a, b**). Accordingly, the Th17/Treg ratio, a well-known marker of GALT integrity and immunological function, also decreased in untreated chronically HIV-infected individuals versus uninfected participants (Mann-Whitney p=0.003), while restored by early but not delayed ART (Fig. 5**c**). Interestingly, ECs, with the longest duration of the infection, had the lowest Th17 cell frequencies and Th17/Treg ratio among the study groups (Fig. 5**b, c**). In this sense, a negative correlation was observed between the Th17/Treg ratio and the duration of the infection (Fig. 5**d**). Accordingly, in ECs, a negative correlation between the frequencies of Th17 cells and the duration of the infection was also detected (Fig. 5**e**). Our data demonstrated that early ART initiation but not the duration of ART (Fig 5**c; Table 3**) normalized the Th17/Treg ratio.

3.7. Early ART failed to decrease the expansion of peripheral pTregs

As Tregs can either be differentiated in the thymus (tTregs) or in the peripheral tissues (pTregs) during inflammation [2], to assess their origin we evaluated the expression of CD31, a marker of recently thymic migrated CD4 T-cells [65], and Helios, a well-known specific marker of thymic Tregs [66,67] (Fig. 6**a**). We observed an increase in the frequencies of $CD31^-FoxP3^+$ and $Helios^-FoxP3^+$ CD4 T-cells overtime during HIV infection (cross-sectional acute *versus* uninfected Mann-Whitney p=0.03 and p=0.002, respectively), suggesting increases in pTreg differentiation, whereas $Helios^-FoxP3^+$ CD4 T-cells was not normalized by early ART initiation (Fig. 6**c, e**). We also observed an increasing trend in the frequencies of thymic $Helios^+FoxP3^+$ and $CD31^+FoxP3^+$ CD4 T-cells following HIV infection, while only $Helios^+FoxP3^+$ were normalized after early ART (Fig. 6**d, e**). Additionally, the frequencies of $CD31^-FoxP3^+$ and $Helios^-FoxP3^+$ pTregs were correlated positively with VL and negatively with CD4/CD8 ratio, suggesting the expansion of pTregs along with disease progression (**Supplementary Fig. 6**). Interestingly, ECs and ICs had significantly lower frequencies of both tTregs and pTregs compared to untreated HIV-infected individuals and uninfected controls (Fig. 6). In line with the increased extrathymic generation of Tregs, which are

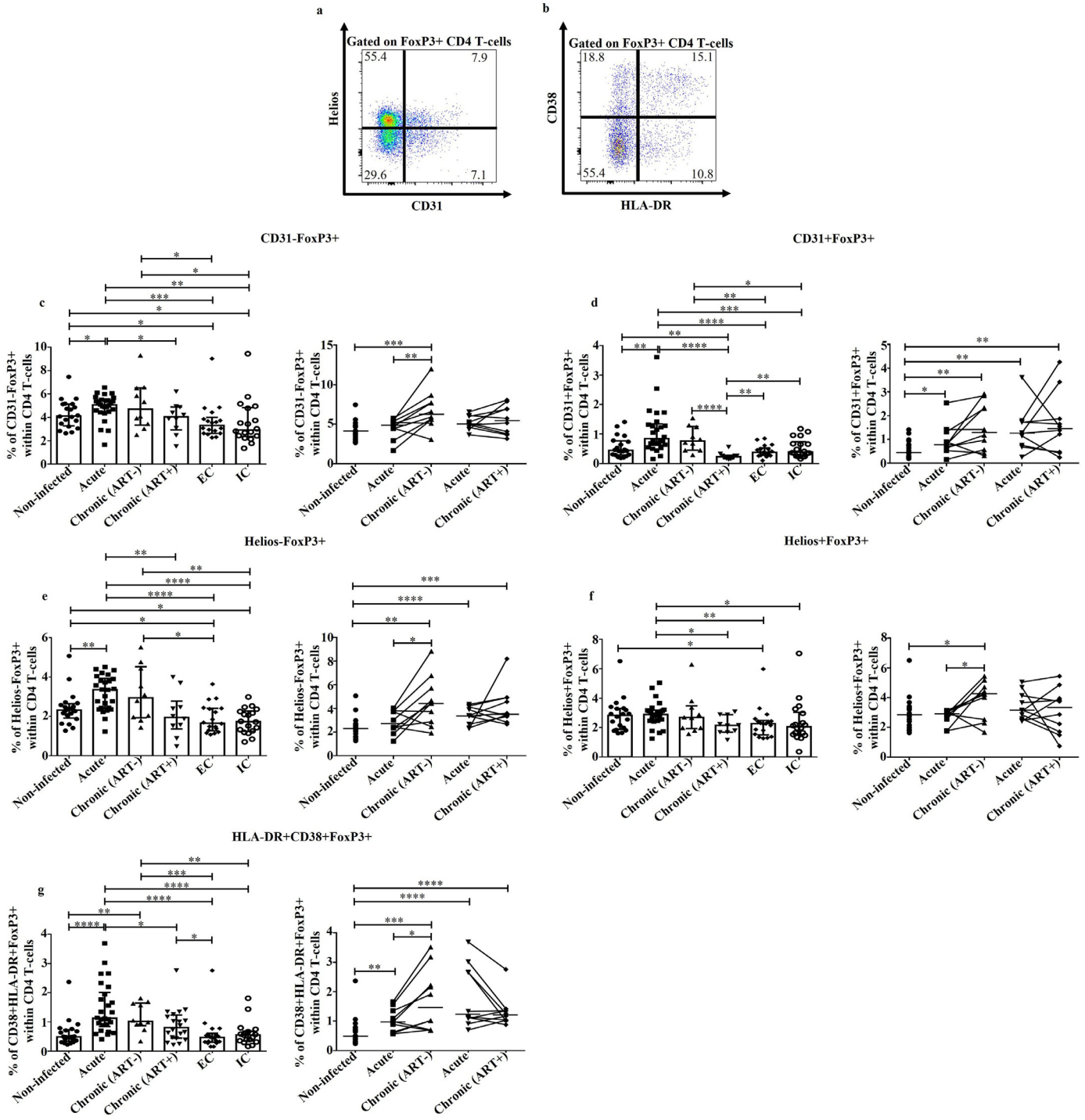

Figure 6. Tregs origin and immune activation overtime during HIV infection and following early ART. (**a**) Gating strategies used to define CD31$^+$, CD31$^-$, Helios$^-$, Helios$^+$ FoxP3$^+$ CD4 T-cells. (b) Gating strategies used to define activated FoxP3$^+$ CD4 T-cells (HLA-DR$^+$CD38$^+$FoxP3$^+$). (**c**) Percentages of CD31$^-$FoxP3$^+$ within CD4 T-cells. (**d**) Percentages of CD31$^+$FoxP3$^+$ within CD4 T-cells. (**e**) Percentages of Helios$^-$FoxP3$^+$ within CD4 T-cells. (**f**) Percentages of Helios$^+$FoxP3$^+$ within CD4 T-cells. (**g**) Percentages of HLA-DR$^+$CD38$^+$FoxP3$^+$ within CD4 T-cells. Statistical significance is indicated in the figures (*, $P < 0.05$; **, $P < 0.01$; ***, $P < 0.001$; ****, $P < 0.0001$). Differences among six study groups was determined by nonparametric Mann-Whitney rank test for unpaired variables, while the Wilcoxon rank tests were used for paired variables in the follow-up study. Sample size in Cross-sectional analysis: non-infected n=20, Acute n=26, Chronic ART- n=10, Chronic ART+ n=11, EC n=18, IC n=18; Sample size in longitudinal analysis: non-infected n=20, ART- n=10, ART+ n=10.

mainly induced during inflammation, we observed increased immune activation of FoxP3$^+$ CD4 T-cells (HLA-DR$^+$CD38$^+$) in untreated HIV-infected individuals that was not reduced following early ART initiation (Fig. 6**a, g**). Moreover, we observed that long-term ART was associated with a decrease in pTregs (Helios$^-$FoxP3$^+$) and activated Tregs (HLA-DR$^+$CD38$^+$FoxP3$^+$), while no correlation was observed on thymic Tregs (Helios$^+$FoxP3$^+$) (Table 3). ECs and ICs had lower levels of Treg immune activation than other HIV-infected individuals (Fig. 6**g**). Altogether, early ART initiation failed to decrease pTreg expansion and Treg immune activation.

Table 4
Demethylation levels of CpG sites at regulatory regions of *foxp3* locus.

Region	Percentage (%) of demethylation						*p*-values
	HIV-non infected(n= 11)	Acute(n= 26)	Chronic ART-(n= 6)	Chronic ART+(n= 77)	EC(n= 10)	IC(n= 10)	
Enhancer Median [IQR]	99 [98-99]	99 [98-100]	99 [97.5-99.25]	99 [99-99]	99.5 [98.75-100]	99 [98-99.25]	0.76
Proximal promoter Median [IQR]	97 [93-100]	97.5 [85-100]	98 [96-99.25]	99 [97-100]	98 [96.5-100]	98.5 [95.5-99.25]	0.85
CNS0 Median [IQR]	85 [84-88]	82 [77-89]	86 [82-90.25]	85 [83-89]	86.5 [77.5-89.75]	83.5 [80.5-84.75]	0.50
CNS2 Median [IQR]	82 [75-96]	78 [53.75-99]	94 [78.25-98.25]	89 [44-92]	90.5 [47.25-96]	87 [81-93.5]	0.86
CNS3 Median [IQR]	96 [95-99]	97 [92.5-99]	98 [97-100]	98 [95-98]	96.5 [85-99.25]	97.5 [94.75-98.25]	0.56

Percentage of CpG demethylation was determined by bisulfite conversion and next generation sequencing of genomic DNA from $CD4^+FoxP3^+$ T cells on six regulatory regions: enhancer, proximal promoter, CNS0, CNS1, CNS2, and CNS3. Results are shown as median and interquartile range (IQR) of percentage of demethylation, and on average 30000 mapped reads were analyzed for each sample.
p-values come from comparing the six groups using the Kruskal-Wallis test.

3.8. Early ART initiation normalized the CpG demethylation status of CNS1 region of the foxp3 *gene*

Methylation of the *foxp3* gene has an essential role in transcription of the gene, which further translates to cell phenotype and activity[68]. We thus evaluated the methylation status of the six regulatory regions of the *foxp3* gene in FACS-sorted $CD4^+FoxP3^+$ cells (**Supplementary Fig. 1).** CNS0, CNS2, CNS3, enhancer, and proximal promoter were highly demethylated among study groups, and no significant differences were observed in sorted cells (**Table 4**). In contrast, and in line with the observed expansion of pTregs overtime of the infection (**Fig. 6**), increases in CNS1 demethylation status were observed in untreated chronically HIV-infected individuals versus uninfected individuals (Mann-Whitney p=0.007) while early ART initiation normalized the levels of CNS1 demethylation (**Fig. 7a**). Additionally, no correlation was observed between the duration of ART and CNS1 demethylation (**Table 3**).

4. Discussion

Early ART initiation as close as possible to the estimated time of HIV exposure is highly recommended in clinical practice due to its proven benefits in facilitating CD4 T-cell count recovery, decreasing immune activation, and reducing secondary HIV transmission [43,46]. The GALT represents one of the major sites of SIV/HIV replication, CD4 depletion, and immune dysfunction [2,34,42-45]. Our team and others have previously shown that GALT fibrosis and microbial translocation start early following HIV/SIV infections along with increased frequencies of immunosuppressive Tregs and TGF-β1 production [28,30,41,69-71]. Herein, we assessed the impact of early ART initiation and duration of ART on the dynamics of Treg immunomodulatory subsets.

Similar to other studies [2,10,28], we observed increased frequencies of total $CD4^+CD25^{high}CD127^{low}FoxP3^+$ Tregs in untreated HIV-infected individuals, which were normalized by early ART, while ECs showed lower Tregs frequencies than HIV-progressors and similar to uninfected individuals [18,72-75]. A distinctive differentiation

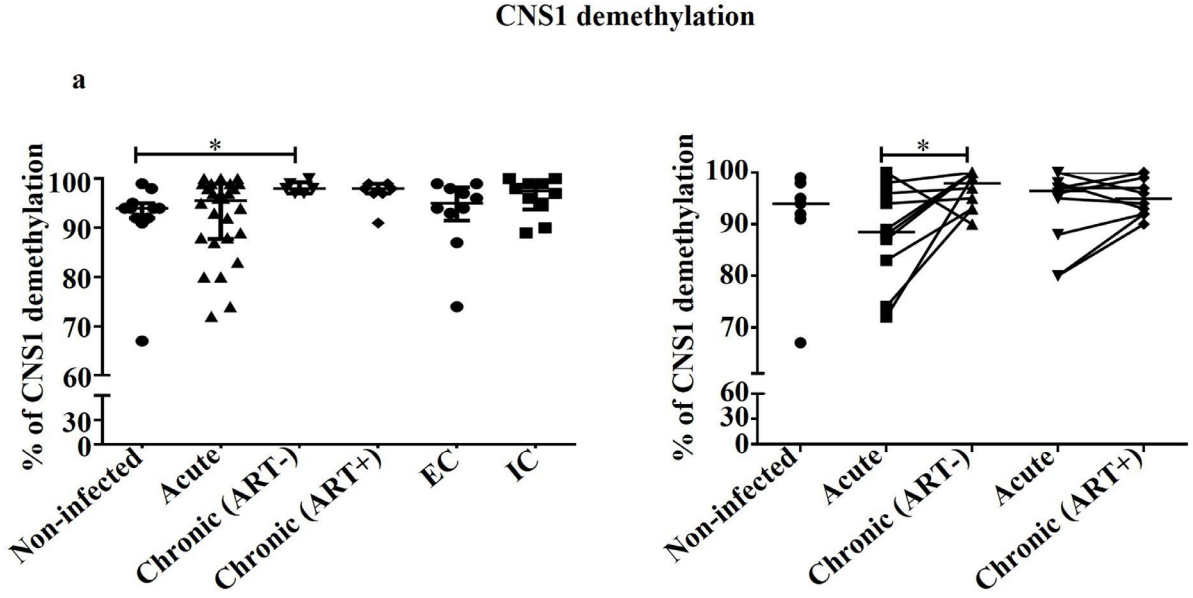

Figure 7. Impact of early ART on CpG sites demethylation of CNS1 region in the *foxp3* gene. (**a**) Percentage of CNS1 demethylation within the *foxp3* gene. Statistical significance is indicated in the figures (*, $P < 0.05$). Differences among six study groups was determined by nonparametric Mann-Whitney rank test for unpaired variables, while the Wilcoxon rank tests were used for paired variables in the follow-up study. Sample size in Cross-sectional analysis: non-infected n=11, Acute n=26, Chronic ART- n=6, Chronic ART+ n=7, EC n=10, IC n=10; Sample size in longitudinal analysis: non-infected n=11, ART- n=10, ART+ n=10.

pattern of Tregs was observed in acute HIV infection, which was characterized by higher proportions of naïve Tregs along with low frequencies of CM and EM Tregs, while in longitudinal analysis early ART initiation didn't affect these subsets. Increase naïve Tregs during untreated infection is likely to be related to a higher thymic output along with the observed increase in Helios^{+}FoxP3^{+} CD4 T-cells over time in our study. This increase in naïve Tregs might also be related to a slow differentiation rate of these cells into CM Tregs during HIV infection [76]. In addition, the low frequencies of CM and EM Tregs in peripheral blood could also indicate higher retention of these cells in lymphoid organs [77,78] or preferential HIV-induced apoptosis of CM Tregs [76].

Early ART had failed to decrease the expression of CTLA4 and PD1 by Tregs which, in turn, might contribute to an increase in Treg-mediated inhibition of effector T-cell proliferation, HIV-specific responses, and cytokine production [1,14,21,22]. Enhanced PD1/PD1L interaction could promote Tregs' development and suppressive functions by stabilizing and maintaining FoxP3 during HIV infection [79-82]. Our study also revealed an increase in memory CTLA4^{+}PD1^{-}FoxP3^{+} T-cells during acute HIV infection. This subset has been recently shown as viral reservoirs in SIV infection during suppressive ART [51], suggesting a potential contribution of Tregs in viral persistence despite early ART. Tregs in EC and IC groups expressed similar CTLA4 levels than uninfected individuals, which could be related to the maintenance of effector cell functions and further better viral control in these individuals compared to HIV progressors.

Increased CD39 expression by Tregs and their production of immunosuppressive adenosine in chronic HIV infection under ART are involved in HIV disease progression [16,26,27,83]. Here, we observed that levels of CD39^{+} Tregs remained higher in blood of ART-treated individuals than uninfected controls. Neither timing of ART initiation, nor duration of ART, were capable of normalizing the frequencies of CD39^{+} Tregs which may contribute to chronic immune dysfunction despite ART, as we previously reported [25,27]. Furthermore, the upregulation of downstream genes of the TGF-β1 pathway occurs as early as one day post-SIV infection of rhesus macaques [84]. We recently showed that early ART initiation at four days post-SIV infection in rhesus macaques is unable to decrease TGF-β1 [28]. Accordingly, here we observed an increase in LAP(TGF-β1)$^{+}$ Tregs during HIV infection that was not restored following ART. Notably, there is a functional positive feedback between CD39 and TGF-β1. CD39 enzymatic activity and the excessive generation of adenosine promote TGF-β1 production and tissue remodelling and fibrosis [85-87], while the TGF-β1 signalling induces CD39 expression and activity [88-91]. The adenosine pathway could also promote the generation of FoxP3^{+} Treg cells [92,93] via the stimulation of TGF-β1 production [31,32]. Importantly, TGF-β1 regulates Treg trafficking to the gut [94,95], and CD39^{+} Tregs maintain their suppressive capacity and exhibit high FoxP3 expression and stability in inflammatory conditions [96].

We found that HIV infection is associated with an early increase in the expression of homing markers CXCR3, CCR6, Integrin β7, and CCR9 by Tregs, which were not normalized by early ART, while negative correlations were observed between their frequencies and duration of ART. Our results are in line with other reports showing increased CXCR3^{+} [97] and Integrin β7^{+} Tregs [98,99] frequencies in HIV-infected individuals and a decrease in small intestinal mucosal CCR6^{+} Treg following ART [100]. We also found that expression of the gut homing markers by CD39^{+} Tregs and LAP(TGF-β1)$^{+}$ Tregs were increased during HIV infection and occurred even in ECs and ICs, but not restored by early ART. This suggests a potential key role of CD39/TGF-β1 interplay in gut mucosal fibrosis and dysfunction, even in the absence of detectable VL.

Altered Th17/Treg balance in favour of Tregs is a main cause of gut mucosal immune dysfunction, which facilitates microbial translocation from gut to peripheral blood, promoting generalized inflammation [47,101-103]. In line with previous reports [28,104,105], we found a decrease in both Th17 cell frequencies and Th17/Treg ratio during HIV infection, while timing of ART initiation but not duration of ART restored Th17/Treg ratio. We also found a lower Th17/Treg ratio in EC versus other HIV-infected individuals or uninfected controls, contrasting with previous reports [74,102,106]. Individuals in the EC group were significantly older than other HIV-infected individuals, which could explain the lower Th17/Treg ratio in these individuals since Th17/Treg balance is disturbed during aging [107]. Besides, we found a negative correlation between the Th17/Treg ratio and the duration of the infection in ECs, suggesting long-term suboptimal immune function and impaired gut barrier functions despite their undetectable viremia [108,109].

To better evaluate the origin of Treg expansion during untreated HIV infection, we assessed the expression of CD31 as a marker of recently thymus emigrant Tregs and Helios, a specific marker of thymic Tregs [65-67]. We observed an increase in CD31^{-} and Helios^{-}FoxP3^{+} CD4 T-cells in untreated HIV infection, while early ART initiation failed to reduce the frequencies of Helios^{-}FoxP3^{+} CD4 T-cells along with the observed increase in the total Treg pool. Additionally, we demonstrated an increase in Helios^{+}FoxP3^{+} CD4 T-cells over time in untreated individuals, indicating increased thymic output of Tregs in these individuals, which was normalized by early ART. Notably, compared to Helios^{-} Tregs, Helios^{+} Tregs are more stable and proliferative *in vivo* and produce high levels of TGF-β1 [110,111]. Significantly, in line with previous reports [23,112], we found that HIV infection was associated with an increase in HLA-DR^{+}CD38^{+} FoxP3^{+} CD4 T-cells, which was not normalized following early ART, and declined along with ART duration. The maintenance of activated FoxP3^{+} CD4 T-cells after early ART is important since this population shows greater suppressive function [113].

For the first time, we assessed the methylation status of the six regulatory regions of *foxp3* locus, i.e., enhancer, proximal promoter, and CNS0-3, to assess the epigenetic regulation of Tregs in HIV infection. We detected significant increases over time only in CNS1 demethylation in untreated HIV-infected individuals that were normalized following early ART initiation. The CNS1 region includes binding sites for several transcription factors, including Smads, nuclear factor of activated T-cells (NFAT), activator protein 1 (AP-1), and retinoic acid receptor (RAR) [7]. Significantly, TGF-β1 induces the binding of Smad2/3 to CNS1 in the *foxp3* locus, which is crucial for FoxP3 induction and differentiation of pTregs [114]. CNS1 demethylation is in line with our finding on the increase in LAP(TGF-β1)$^{+}$ Tregs and expansion of Helios^{-}FoxP3^{+} pTregs in untreated HIV infection. Notably, we did not observe any differences in CNS2 demethylation, a well-known regulatory region that contributes to continuous expression of FoxP3 in tTregs and their stability [115-117], which was in line with frequencies of Helios^{-}FoxP3^{+} tTregs, and with previous reports on rarely CNS2 demethylation in conventional T-cells or TGF-β-induced iTregs generated *in vitro* [116]. We observed higher levels of LAP(TGF-β1)$^{+}$ Tregs in ECs than uninfected individuals, along with no differences in CNS1 demethylation between these two study groups. Our results suggest that other possible mechanisms, in addition to the effect of LAP(TGF-β1) on CNS1 demethylation might be involved in differential Treg homeostasis in ECs [73,74,112]. As such, we previously reported distinct tryptophan catabolism in ECs which is known to be involved in the generation of pTregs in HIV infection [47]. Furthermore, the induction of pTregs is impaired with age, while tTregs are increased with age [118]. Accordingly, the older age in ECs could also explain, partially, the lack of significant difference in CNS1 demethylation in ECs *versus* uninfected individuals.

The findings of this study must be considered in light of some limitations. We acknowledge that confounders such as sex, age, duration of infection and the timing of ART initiation, might impact our observations. Males and persons of older age are known to have higher Tregs frequencies compared to females [119-121] and younger individuals [122-124]. Additionally, sex and age-related differences exist

in the expression of immune checkpoints PD1 and CTLA4 [125,126], and, TGF-β1 [127-130]. In our study, we mainly included male individuals since the majority of participants in the Montreal primary infection (acute) cohort are male. Furthermore, as previously indicated, the methylation status of the *foxp3* gene can be done adequately only in males [49]. The higher proportion of females in the EC and IC groups was due to the availability of these rare specimens and a higher number of women in these study cohorts, which, in turn, might impact some of our observations. The significant older age in both EC and chronic ART$^+$ groups in the cross-sectional study, might also affect our results. As such, the discordances in CTLA4, PD1, CD31 or CCR6 expression by Tregs in ART$^+$ individuals in cross-sectional *versus* longitudinal studies, might be explained by the significantly older age of ART$^+$ individuals in cross-sectional specimens along with their significantly longer duration of infection. We also recognize that the small sample size available for our study is a limitation and would benefit from replication. However, our findings are in keeping with our previous results and have high biological plausibility [47,69,131-134]. Moreover, due to the limited availability of the specimens, we were not able to perform *in vitro* Treg functional assays. Finally, although we used well-known markers of T-cell migration to the gut, all assessments were done in peripheral blood as an indirect indicator of Treg migration into the GALT. Further studies to evaluate the dynamics of Tregs in gut mucosal tissue are needed to confirm our observations.

In summary, we showed that even though early ART initiation clearly improved CD4 recovery and T-cell immune activation and exhaustion, the frequencies of immunosuppressive and pro-fibrogenic Tregs and their potential migration toward the gut overtime were not affected by early ART. Our results suggest that immunotherapies which impact the CD39/TGF-β1 pathway or reduce Treg homing to gut could be tested in clinical trials as adjuncts to ART to prevent gut mucosal fibrosis.

Contributors

MAJ designed the study; AY, TS, OF performed the experiments. JPR, ChT, CT, CTC provided access to specimens and clinical data; AY, TS, OF, MD, CTC, MAJ analysed, discussed, and interpreted results throughout the study. AY and MAJ wrote the paper. All authors contributed to the refinement of the study and reviewed and approved the final version of manuscript. AY, TS, MD and MAJ have verified the underlying data.

Data sharing

Data from this manuscript is available from the corresponding author upon reasonable request

Declaration of Competing Interest

We have no competing of interest to declare.

Acknowledgments

First and foremost, the authors thank all study participants for their time and significant dedication to this study. Subjects in the early phase of infection were screened, recruited, and followed up at the following Montreal-based clinics and we thank for their collaboration: l'Actuel Medical Clinic, Quartier Latin Medical Clinic, UHRESS CHUM Hôtel-Dieu and Notre-Dame; and MUHC Chest Institute. We also thank M. Mario Legault, for administrative support, Ms. Angie Massicotte, for her assistance and coordination; Ms. Loiuse Gilbert for the MUHC biobanking support; and Ms. Stephanie Matte from the Canadian HIV-1 Slow Progressor cohort. This study was funded by the Canadian Institutes of Health Research (CIHR, grant MOP 142294) and in part by the AIDS and Infectious Diseases Network of the *Réseau SIDA et maladies infectieuses du Fonds de recherche du Québec-Santé* (FRQ-S) to MAJ. AY is supported by an FRQ-S doctoral scholarship. JPR holds the McGill University Louis Lowenstein Chair in Hematology and Oncology. CT colds the Pfizer Chair in Clinical and Translational Research on HIV. MD and CTC hold FRQ-S Junior 2 Clinician-researcher career awards. MAJ holds the tier 2 CIHR Canada Research Chair in Immuno-Virology.

Supplementary materials

Supplementary material associated with this article can be found in the online version at doi:10.1016/j.ebiom.2021.103570.

References

[1] Sakaguchi S, Mikami N, Wing JB, Tanaka A, Ichiyama K, Ohkura N. Regulatory T Cells and Human Disease. Annual Review of Immunology 2020;38(1):541–66.
[2] Jenabian MA, Ancuta P, Gilmore N, Routy JP. Regulatory T cells in HIV infection: can immunotherapy regulate the regulator? Clin Dev Immunol 2012;2012:908314.
[3] Josefowicz SZ, Lu LF, Rudensky AY. Regulatory T cells: mechanisms of differentiation and function. Annu Rev Immunol 2012;30:531–64.
[4] Mohr A, Atif M, Balderas R, Gorochov G, Miyara M. The role of FOXP3(+) regulatory T cells in human autoimmune and inflammatory diseases. Clin Exp Immunol 2019;197(1):24–35.
[5] Zheng Y, Josefowicz S, Chaudhry A, Peng XP, Forbush K, Rudensky AY. Role of conserved non-coding DNA elements in the Foxp3 gene in regulatory T-cell fate. Nature 2010;463(7282):808–12.
[6] Mohr A, Malhotra R, Mayer G, Gorochov G, Miyara M. Human FOXP3(+) T regulatory cell heterogeneity. Clin Transl Immunology 2018;7(1):e1005.
[7] Sekiya T, Nakatsukasa H, Lu Q, Yoshimura A. Roles of transcription factors and epigenetic modifications in differentiation and maintenance of regulatory T cells. Microbes Infect 2016;18(6):378–86.
[8] Feng Y, van der Veeken J, Shugay M, Putintseva EV, Osmanbeyoglu HU, Dikiy S, et al. A mechanism for expansion of regulatory T-cell repertoire and its role in self-tolerance. Nature 2015;528(7580):132–6.
[9] Chevalier MF, Didier C, Petitjean G, Karmochkine M, Girard PM, Barre-Sinoussi F, et al. Phenotype alterations in regulatory T-cell subsets in primary HIV infection and identification of Tr1-like cells as the main interleukin 10-producing CD4+ T cells. J Infect Dis 2015;211(5):769–79.
[10] Chevalier MF, Weiss L. The split personality of regulatory T cells in HIV infection. Blood 2013;121(1):29–37.
[11] Kleinman AJ, Sivanandham R, Pandrea I, Chougnet CA. Apetrei C. Regulatory T Cells As Potential Targets for HIV Cure Research. Front Immunol 2018;9:734.
[12] Abdel-Hameed EA, Ji H, Sherman KE, Shata MT. Epigenetic modification of FOXP3 in patients with chronic HIV infection. J Acquir Immune Defic Syndr 2014;65(1):19–26.
[13] Pion M, Jaramillo-Ruiz D, Martinez A, Munoz-Fernandez MA, Correa-Rocha R. HIV infection of human regulatory T cells downregulates Foxp3 expression by increasing DNMT3b levels and DNA methylation in the FOXP3 gene. AIDS 2013;27(13):2019–29.
[14] Qureshi OS, Zheng Y, Nakamura K, Attridge K, Manzotti C, Schmidt EM, et al. Trans-Endocytosis of CD80 and CD86: A Molecular Basis for the Cell-Extrinsic Function of CTLA-4. Science 2011;332(6029):600–3.
[15] Wing K, Onishi Y, Prieto-Martin P, Yamaguchi T, Miyara M, Fehervari Z, et al. CTLA-4 control over Foxp3+ regulatory T cell function. Science 2008;322 (5899):271–5.
[16] Schulze Zur Wiesch J, Thomssen A, Hartjen P, Toth I, Lehmann C, Meyer-Olson D, et al. Comprehensive analysis of frequency and phenotype of T regulatory cells in HIV infection: CD39 expression of FoxP3+ T regulatory cells correlates with progressive disease. J Virol 2011;85(3):1287–97.
[17] Vallejo A, Abad-Fernandez M, Moreno S, Moreno A, Perez-Elias MJ, Dronda F, et al. High levels of CD4(+) CTLA-4(+) Treg cells and CCR5 density in HIV-1-infected patients with visceral leishmaniasis. Eur J Clin Microbiol Infect Dis 2015;34(2):267–75.
[18] Rueda CM, Velilla PA, Chougnet CA, Rugeles MT. Incomplete normalization of regulatory t-cell frequency in the gut mucosa of Colombian HIV-infected patients receiving long-term antiretroviral treatment. PLoS One 2013;8(8): e71062.
[19] Francisco LM, Sage PT, Sharpe AH. The PD-1 pathway in tolerance and autoimmunity. Immunological Reviews 2010;236(1):219–42.
[20] Rodriguez-Perea AL, Arcia ED, Rueda CM, Velilla PA. Phenotypical characterization of regulatory T cells in humans and rodents. Clin Exp Immunol 2016;185 (3):281–91.
[21] Asano T, Kishi Y, Meguri Y, Yoshioka T, Iwamoto M, Maeda Y, et al. PD-1 Signaling Has a Critical Role in Maintaining Regulatory T Cell Homeostasis; Implication for Treg Depletion Therapy By PD-1 Blockade. Blood 2015;126(23):848.
[22] Zhang B, Chikuma S, Hori S, Fagarasan S, Honjo T. Nonoverlapping roles of PD-1 and FoxP3 in maintaining immune tolerance in a novel autoimmune pancreatitis mouse model. Proc Natl Acad Sci U S A. 2016;113(30):8490–5.

[23] Xiao J, Zhang L, Dong Y, Liu X, Peng L, Yang Y, et al. PD-1 Upregulation Is Associated with Exhaustion of Regulatory T Cells and Reflects Immune Activation in HIV-1-Infected Individuals. AIDS Res Hum Retroviruses 2019;35(5):444–52.
[24] Deaglio S, Dwyer KM, Gao W, Friedman D, Usheva A, Erat A, et al. Adenosine generation catalyzed by CD39 and CD73 expressed on regulatory T cells mediates immune suppression. J Exp Med 2007;204(6):1257–65.
[25] Jenabian MA, Seddiki N, Yatim A, Carriere M, Hulin A, Younas M, et al. Regulatory T cells negatively affect IL-2 production of effector T cells through CD39/adenosine pathway in HIV infection. PLoS Pathog 2013;9(4):e1003319.
[26] Presicce P, Orsborn K, King E, Pratt J, Fichtenbaum CJ, Chougnet CA. Frequency of circulating regulatory T cells increases during chronic HIV infection and is largely controlled by highly active antiretroviral therapy. PLoS One 2011;6(12):e28118.
[27] Nikolova M, Carriere M, Jenabian MA, Limou S, Younas M, Kok A, et al. CD39/adenosine pathway is involved in AIDS progression. PLoS Pathog 2011;7(7):e1002110.
[28] Yero A, Farnos O, Rabezanahary H, Racine G, Estaquier J, Jenabian MA. Differential Dynamics of Regulatory T-Cell and Th17 Cell Balance in Mesenteric Lymph Nodes and Blood following Early Antiretroviral Initiation during Acute Simian Immunodeficiency Virus Infection. J Virol 2019;93(19).
[29] Estes JD, Wietgrefe S, Schacker T, Southern P, Beilman G, Reilly C, et al. Simian immunodeficiency virus-induced lymphatic tissue fibrosis is mediated by transforming growth factor beta 1-positive regulatory T cells and begins in early infection. J Infect Dis 2007;195(4):551–61.
[30] Zeng M, Smith AJ, Wietgrefe SW, Southern PJ, Schacker TW, Reilly CS, et al. Cumulative mechanisms of lymphoid tissue fibrosis and T cell depletion in HIV-1 and SIV infections. J Clin Invest 2011;121(3):998–1008.
[31] Li MO, Wan YY, Sanjabi S, Robertson AK, Flavell RA. Transforming growth factor-beta regulation of immune responses. Annu Rev Immunol 2006;24:99–146.
[32] Chen W, Jin W, Hardegen N, Lei KJ, Li L, Marinos N, et al. Conversion of peripheral CD4+CD25- naive T cells to CD4+CD25+ regulatory T cells by TGF-beta induction of transcription factor Foxp3. J Exp Med 2003;198(12):1875–86.
[33] Ahmadzadeh M, Rosenberg SA. TGF-beta 1 attenuates the acquisition and expression of effector function by tumor antigen-specific human memory CD8 T cells. J Immunol 2005;174(9):5215–23.
[34] Cumont MC, Monceaux V, Viollet L, Lay S, Parker R, Hurtrel B, et al. TGF-beta in intestinal lymphoid organs contributes to the death of armed effector CD8 T cells and is associated with the absence of virus containment in rhesus macaques infected with the simian immunodeficiency virus. Cell Death Differ 2007;14(10):1747–58.
[35] Schacker TW, Nguyen PL, Beilman GJ, Wolinsky S, Larson M, Reilly C, et al. Collagen deposition in HIV-1 infected lymphatic tissues and T cell homeostasis. J Clin Invest 2002;110(8):1133–9.
[36] Klatt NR, Chomont N, Douek DC. Deeks SG. Immune activation and HIV persistence: implications for curative approaches to HIV infection. Immunol Rev 2013;254(1):326–42.
[37] Pandrea I, Landay A, Wilson C, Stock J, Tracy R, Apetrei C. Using the pathogenic and nonpathogenic nonhuman primate model for studying non-AIDS comorbidities. Curr HIV/AIDS Rep 2015;12(1):54–67.
[38] Sandler NG, Douek DC. Microbial translocation in HIV infection: causes, consequences and treatment opportunities. Nature reviews Microbiology 2012;10(9):655–66.
[39] Vyboh K, Jenabian MA, Mehraj V, Routy JP. HIV and the gut microbiota, partners in crime: breaking the vicious cycle to unearth new therapeutic targets. Journal of immunology research 2015;2015:614127.
[40] Caetano DG, de Paula HHS, Bello G, Hoagland B, Villela LM, Grinsztejn B, et al. HIV-1 elite controllers present a high frequency of activated regulatory T and Th17 cells. PLoS One 2020;15(2):e0228745.
[41] Sanchez JL, Hunt PW, Reilly CS, Hatano H, Beilman GJ, Khoruts A, et al. Lymphoid fibrosis occurs in long-term nonprogressors and persists with antiretroviral therapy but may be reversible with curative interventions. J Infect Dis 2015;211(7):1068–75.
[42] Gosselin A, Wiche Salinas TR, Planas D, Wacleche VS, Zhang Y, Fromentin R, et al. HIV persists in CCR6+CD4+ T cells from colon and blood during antiretroviral therapy. AIDS 2017;31(1):35–48.
[43] Maartens G, Celum C, Lewin SR. HIV infection: epidemiology, pathogenesis, treatment, and prevention. Lancet 2014;384(9939):258–71.
[44] McGary CS, Alvarez X, Harrington S, Cervasi B, Ryan ES, Iriele RI, et al. The loss of CCR6(+) and CD161(+) CD4(+) T-cell homeostasis contributes to disease progression in SIV-infected rhesus macaques. Mucosal Immunol 2017;10(4):1082–96.
[45] Khoury G, Fromentin R, Solomon A, Hartogensis W, Killian M, Hoh R, et al. Human Immunodeficiency Virus Persistence and T-Cell Activation in Blood, Rectal, and Lymph Node Tissue in Human Immunodeficiency Virus-Infected Individuals Receiving Suppressive Antiretroviral Therapy. J Infect Dis 2017;215(6):911–9.
[46] Rajasuriar R, Wright E, Lewin SR. Impact of antiretroviral therapy (ART) timing on chronic immune activation/inflammation and end-organ damage. Curr Opin HIV AIDS 2015;10(1):35–42.
[47] Jenabian MA, Patel M, Kema I, Kanagaratham C, Radzioch D, Thebault P, et al. Distinct tryptophan catabolism and Th17/Treg balance in HIV progressors and elite controllers. PLoS One 2013;8(10):e78146.
[48] Zeng M, Southern PJ, Reilly CS, Beilman GJ, Chipman JG, Schacker TW, et al. Lymphoid tissue damage in HIV-1 infection depletes naive T cells and limits T cell reconstitution after antiretroviral therapy. PLoS Pathog 2012;8(1):e1002437.
[49] Wieczorek G, Asemissen A, Model F, Turbachova I, Floess S, Liebenberg V, et al. Quantitative DNA methylation analysis of FOXP3 as a new method for counting regulatory T cells in peripheral blood and solid tissue. Cancer Res 2009;69(2):599–608.
[50] Huehn J, Polansky JK, Hamann A. Epigenetic control of FOXP3 expression: the key to a stable regulatory T-cell lineage? Nat Rev Immunol 2009;9(2):83–9.
[51] McGary CS, Deleage C, Harper J, Micci L, Ribeiro SP, Paganini S, et al. CTLA-4(+)PD-1(-) Memory CD4(+) T Cells Critically Contribute to Viral Persistence in Antiretroviral Therapy-Suppressed, SIV-Infected Rhesus Macaques. Immunity 2017;47(4):776–88 e5.
[52] Kim KK, Sheppard D, Chapman HA. TGF-β1 Signaling and Tissue Fibrosis. Cold Spring Harb Perspect Biol 2018;10(4):a022293.
[53] Hasegawa H, Inoue A, Kohno M, Lei J, Miyazaki T, Yoshie O, et al. Therapeutic effect of CXCR3-expressing regulatory T cells on liver, lung and intestinal damages in a murine acute GVHD model. Gene Therapy 2008;15(3):171–82.
[54] Chow Z, Banerjee A, Hickey MJ. Controlling the fire–tissue-specific mechanisms of effector regulatory T-cell homing. Immunol Cell Biol 2015;93(4):355–63.
[55] Yamazaki T, Yang XO, Chung Y, Fukunaga A, Nurieva R, Pappu B, et al. CCR6 regulates the migration of inflammatory and regulatory T cells. J Immunol 2008;181(12):8391–401.
[56] Berlin C, Berg EL, Briskin MJ, Andrew DP, Kilshaw PJ, Holzmann B, et al. Alpha 4 beta 7 integrin mediates lymphocyte binding to the mucosal vascular addressin MAdCAM-1. Cell 1993;74(1):185–95.
[57] Wagner N, Löhler J, Kunkel EJ, Ley K, Leung E, Krissansen G, et al. Critical role for beta7 integrins in formation of the gut-associated lymphoid tissue. Nature 1996;382(6589):366–70.
[58] Sun H, Kuk W, Rivera-Nieves J, Lopez-Ramirez MA, Eckmann L, Ginsberg MH. beta7 Integrin Inhibition Can Increase Intestinal Inflammation by Impairing Homing of CD25(hi)FoxP3(+) Regulatory T Cells. Cell Mol Gastroenterol Hepatol 2020;9(3):369–85.
[59] Zhang HL, Zheng YJ, Pan YD, Xie C, Sun H, Zhang YH, et al. Regulatory T-cell depletion in the gut caused by integrin beta7 deficiency exacerbates DSS colitis by evoking aberrant innate immunity. Mucosal Immunol 2016;9(2):391–400.
[60] Pabst O. Trafficking of regulatory T cells in the intestinal immune system. Int Immunol 2013;25(3):139–43.
[61] Uehara S, Grinberg A, Farber JM, Love PE. A Role for CCR9 in T Lymphocyte Development and Migration. The Journal of Immunology 2002;168(6):2811–9.
[62] Hoeppli RE, MacDonald KN, Leclair P, Fung VCW, Mojibian M, Gillies J, et al. Tailoring the homing capacity of human Tregs for directed migration to sites of Th1-inflammation or intestinal regions. Am J Transplant 2019;19(1):62–76.
[63] Gosselin A, Monteiro P, Chomont N, Diaz-Griffero F, Said EA, Fonseca S, et al. Peripheral blood CCR4+CCR6+ and CXCR3+CCR6+CD4+ T cells are highly permissive to HIV-1 infection. J Immunol 2010;184(3):1604–16.
[64] Monteiro P, Gosselin A, Wacleche VS, El-Far M, Said EA, Kared H, et al. Memory CCR6+CD4+ T cells are preferential targets for productive HIV type 1 infection regardless of their expression of integrin beta7. J Immunol 2011;186(8):4618–30.
[65] Douaisi M, Resop RS, Nagasawa M, Craft J, Jamieson BD, Blom B, et al. CD31, a Valuable Marker to Identify Early and Late Stages of T Cell Differentiation in the Human Thymus. J Immunol 2017;198(6):2310–9.
[66] Takatori H, Kawashima H, Matsuki A, Meguro K, Tanaka S, Iwamoto T, et al. Helios Enhances Treg Cell Function in Cooperation With FoxP3. Arthritis Rheumatol 2015;67(6):1491–502.
[67] Thornton AM, Korty PE, Tran DQ, Wohlfert EA, Murray PE, Belkaid Y, et al. Expression of Helios, an Ikaros transcription factor family member, differentiates thymic-derived from peripherally induced Foxp3+ T regulatory cells. J Immunol 2010;184(7):3433–41.
[68] Sakai R, Komai K, Iizuka-Koga M, Yoshimura A, Ito M. Regulatory T Cells: Pathophysiological Roles and Clinical Applications. Keio J Med 2020;69(1):1–15.
[69] Jenabian MA, El-Far M, Vyboh K, Kema I, Costiniuk CT, Thomas R, et al. Immunosuppressive Tryptophan Catabolism and Gut Mucosal Dysfunction Following Early HIV Infection. J Infect Dis 2015;212(3):355–66.
[70] Andersson J, Boasso A, Nilsson J, Zhang R, Shire NJ, Lindback S, et al. The prevalence of regulatory T cells in lymphoid tissue is correlated with viral load in HIV-infected patients. J Immunol 2005;174(6):3143–7.
[71] Nilsson J, Boasso A, Velilla PA, Zhang R, Vaccari M, Franchini G, et al. HIV-1-driven regulatory T-cell accumulation in lymphoid tissues is associated with disease progression in HIV/AIDS. Blood 2006;108(12):3808–17.
[72] Shaw JM, Hunt PW, Critchfield JW, McConnell DH, Garcia JC, Pollard RB, et al. Increased frequency of regulatory T cells accompanies increased immune activation in rectal mucosae of HIV-positive noncontrollers. J Virol 2011;85(21):11422–34.
[73] Hunt PW, Landay AL, Sinclair E, Martinson JA, Hatano H, Emu B, et al. A low T regulatory cell response may contribute to both viral control and generalized immune activation in HIV controllers. PLoS One 2011;6(1):e15924.
[74] Brandt L, Benfield T, Mens H, Clausen LN, Katzenstein TL, Fomsgaard A, et al. Low level of regulatory T cells and maintenance of balance between regulatory T cells and TH17 cells in HIV-1-infected elite controllers. J Acquir Immune Defic Syndr 2011;57(2):101–8.
[75] Rios CM, Velilla PA, Rugeles MT. Chronically HIV-1 Infected Patients Exhibit Low Frequencies of CD25+ Regulatory T Cells. Open Virol J 2012;6:49–58.
[76] Oswald-Richter K, Grill SM, Shariat N, Leelawong M, Sundrud MS, Haas DW, et al. HIV infection of naturally occurring and genetically reprogrammed human regulatory T-cells. PLoS Biol 2004;2(7):E198.
[77] Menning A, Hopken UE, Siegmund K, Lipp M, Hamann A, Huehn J. Distinctive role of CCR7 in migration and functional activity of naive- and effector/memory-like Treg subsets. Eur J Immunol 2007;37(6):1575–83.
[78] Masopust D, Vezys V, Marzo AL, Lefrançois L. Preferential localization of effector memory cells in nonlymphoid tissue. Science 2001;291(5512):2413–7.

[79] Wölfle SJ, Strebovsky J, Bartz H, Sähr A, Arnold C, Kaiser C, et al. PD-L1 expression on tolerogenic APCs is controlled by STAT-3. Eur J Immunol 2011;41(2):413–24.
[80] Francisco LM, Salinas VH, Brown KE, Vanguri VK, Freeman GJ, Kuchroo VK, et al. PD-L1 regulates the development, maintenance, and function of induced regulatory T cells. J Exp Med 2009;206(13):3015–29.
[81] Chen X, Fosco D, Kline DE, Meng L, Nishi S, Savage PA, et al. PD-1 regulates extrathymic regulatory T-cell differentiation. Eur J Immunol 2014;44(9):2603–16.
[82] Dong Y, Han Y, Huang Y, Jiang S, Huang Z, Chen R, et al. PD-L1 Is Expressed and Promotes the Expansion of Regulatory T Cells in Acute Myeloid Leukemia. Frontiers in Immunology 2020;11(1710).
[83] Burton CT, Westrop SJ, Eccles-James I, Boasso A, Nelson MR, Bower M, et al. Altered phenotype of regulatory T cells associated with lack of human immunodeficiency virus (HIV)-1-specific suppressive function. Clin Exp Immunol 2011;166(2):191–200.
[84] Barouch DH, Ghneim K, Bosche WJ, Li Y, Berkemeier B, Hull M, et al. Rapid Inflammasome Activation following Mucosal SIV Infection of Rhesus Monkeys. Cell 2016;165(3):656–67.
[85] Wen J, Jiang X, Dai Y, Zhang Y, Tang Y, Sun H, et al. Increased adenosine contributes to penile fibrosis, a dangerous feature of priapism, via A2B adenosine receptor signaling. The FASEB Journal 2010;24(3):740–9.
[86] Luo F, Le N-B, Mills T, Chen N-Y, Karmouty-Quintana H, Molina JG, et al. Extracellular adenosine levels are associated with the progression and exacerbation of pulmonary fibrosis. The FASEB Journal 2016;30(2):874–83.
[87] Künzli BM, Nuhn P, Enjyoji K, Banz Y, Smith RN, Csizmadia E, et al. Disordered Pancreatic Inflammatory Responses and Inhibition of Fibrosis in CD39-Null Mice. Gastroenterology 2008;134(1):292–305.
[88] Peres RS, Donate PB, Talbot J, Cecilio NT, Lobo PR, Machado CC, et al. TGF-β signalling defect is linked to low CD39 expression on regulatory T cells and methotrexate resistance in rheumatoid arthritis. Journal of Autoimmunity 2018;90:49–58.
[89] Ye Z-J, Zhou Q, Zhang J-C, Li X, Wu C, Qin S-M, et al. CD39+Regulatory T cells suppress generation and differentiation of Th17 cells in human malignant pleural effusion via a LAP-dependent mechanism. Respiratory Research 2011;12(1):77.
[90] Regateiro FS, Howie D, Nolan KF, Agorogiannis EI, Greaves DR, Cobbold SP, et al. Generation of anti-inflammatory adenosine byleukocytes is regulated by TGF-β. European Journal of Immunology 2011;41(10):2955–65.
[91] Gerner MC, Ziegler LS, Schmidt RLJ, Krenn M, Zimprich F, Uyanik-Ünal K, et al. The TGF-b/SOX4 axis and ROS-driven autophagy co-mediate CD39 expression in regulatory T-cells. The FASEB Journal 2020;34(6):8367–84.
[92] Zarek PE, Huang C-T, Lutz ER, Kowalski J, Horton MR, Linden J, et al. A2A receptor signaling promotes peripheral tolerance by inducing T-cell anergy and the generation of adaptive regulatory T cells. Blood 2008;111(1):251–9.
[93] Ohta A, Kini R, Ohta A, Subramanian M, Madasu M, Sitkovsky M. The development and immunosuppressive functions of CD4+ CD25+ FoxP3+ regulatory T cells are under influence of the adenosine-A2A adenosine receptor pathway. Frontiers in Immunology 2012;3(190).
[94] Kim SV, Xiang WV, Kwak C, Yang Y, Lin XW, Ota M, et al. GPR15-mediated homing controls immune homeostasis in the large intestine mucosa. Science 2013;340(6139):1456–9.
[95] Konkel JE, Zhang D, Zanvit P, Chia C, Zangarle-Murray T, Jin W, et al. Transforming Growth Factor-β Signaling in Regulatory T Cells Controls T Helper-17 Cells and Tissue-Specific Immune Responses. Immunity 2017;46(4):660–74.
[96] Gu J, Ni X, Pan X, Lu H, Lu Y, Zhao J, et al. Human CD39(hi) regulatory T cells present stronger stability and function under inflammatory conditions. Cell Mol Immunol 2017;14(6):521–8.
[97] Matavele Chissumba R, Namalango E, Maphossa V, Macicame I, Bhatt N, Polyak C, et al. Helios + Regulatory T cell frequencies are correlated with control of viral replication and recovery of absolute CD4 T cells counts in early HIV-1 infection. BMC Immunol 2017;18(1):50.
[98] Ji J, Cloyd MW. HIV-1 binding to CD4 on CD4+CD25+ regulatory T cells enhances their suppressive function and induces them to home to, and accumulate in, peripheral and mucosal lymphoid tissues: an additional mechanism of immunosuppression. Int Immunol 2009;21(3):283–94.
[99] Lu X, Li Z, Li Q, Jiao Y, Ji Y, Zhang H, et al. Preferential loss of gut-homing alpha4-beta7 CD4(+) T cells and their circulating functional subsets in acute HIV-1 infection. Cell Mol Immunol 2016;13(6):776–84.
[100] Loiseau C, Requena M, Mavigner M, Cazabat M, Carrere N, Suc B, et al. CCR6(-) regulatory T cells blunt the restoration of gut Th17 cells along the CCR6-CCL20 axis in treated HIV-1-infected individuals. Mucosal Immunol 2016;9(5):1137–50.
[101] Kanwar B, Favre D, McCune JM. Th17 and regulatory T cells: implications for AIDS pathogenesis. Curr Opin HIV AIDS 2010;5(2):151–7.
[102] Favre D, Lederer S, Kanwar B, Ma ZM, Proll S, Kasakow Z, et al. Critical loss of the balance between Th17 and T regulatory cell populations in pathogenic SIV infection. PLoS Pathog 2009;5(2):e1000295.
[103] Kim CJ, McKinnon LR, Kovacs C, Kandel G, Huibner S, Chege D, et al. Mucosal Th17 cell function is altered during HIV infection and is an independent predictor of systemic immune activation. J Immunol 2013;191(5):2164–73.
[104] Schuetz A, Deleage C, Sereti I, Rerknimitr R, Phanuphak N, Phuang-Ngern Y, et al. Initiation of ART during early acute HIV infection preserves mucosal Th17 function and reverses HIV-related immune activation. PLoS Pathog 2014;10(12):e1004543.
[105] Caruso MP, Falivene J, Holgado MP, Zurita DH, Laufer N, Castro C, et al. Impact of HIV-ART on the restoration of Th17 and Treg cells in blood and female genital mucosa. Sci Rep 2019;9(1):1978.
[106] Falivene J, Ghiglione Y, Laufer N, Socías ME, Holgado MP, Ruiz MJ, et al. Th17 and Th17/Treg ratio at early HIV infection associate with protective HIV-specific CD8 + T-cell responses and disease progression. Scientific Reports 2015;5(1):11511.
[107] Schmitt V, Rink L, Uciechowski P. The Th17/Treg balance is disturbed during aging. Exp Gerontol 2013;48(12):1379–86.
[108] Gonzalez SM, Taborda NA, Correa LA, Castro GA, Hernandez JC, Montoya CJ, et al. Particular activation phenotype of T cells expressing HLA-DR but not CD38 in GALT from HIV-controllers is associated with immune regulation and delayed progression to AIDS. Immunol Res 2016;64(3):765–74.
[109] Hatano H, Somsouk M, Sinclair E, Harvill K, Gilman L, Cohen M, et al. Comparison of HIV DNA and RNA in gut-associated lymphoid tissue of HIV-infected controllers and noncontrollers. AIDS 2013;27(14):2255–60.
[110] Sebastian M, Lopez-Ocasio M, Metidji A, Rieder SA, Shevach EM, Thornton AM. Helios Controls a Limited Subset of Regulatory T Cell Functions. J Immunol 2016;196(1):144–55.
[111] Zabransky DJ, Nirschl CJ, Durham NM, Park BV, Ceccato CM, Bruno TC, et al. Phenotypic and functional properties of Helios+ regulatory T cells. PLoS One 2012;7(3):e34547.
[112] Shahbaz S, Jovel J, Elahi S. Differential transcriptional and functional properties of regulatory T cells in HIV-infected individuals on antiretroviral therapy and long-term non-progressors. Clin Transl Immunology 2021;10(5):e1289.
[113] Chen X, Oppenheim JJ. Resolving the identity myth: key markers of functional CD4+FoxP3+ regulatory T cells. Int Immunopharmacol 2011;11(10):1489–96.
[114] Iizuka-Koga M, Nakatsukasa H, Ito M, Akanuma T, Lu Q, Yoshimura A. Induction and maintenance of regulatory T cells by transcription factors and epigenetic modifications. J Autoimmun 2017;83:113–21.
[115] Li X, Liang Y, LeBlanc M, Benner C, Zheng Y. Function of a Foxp3 cis-element in protecting regulatory T cell identity. Cell 2014;158(4):734–48.
[116] Floess S, Freyer J, Siewert C, Baron U, Olek S, Polansky J, et al. Epigenetic control of the foxp3 locus in regulatory T cells. PLoS Biol 2007;5(2):e38.
[117] Rubtsov YP, Niec RE, Josefowicz S, Li L, Darce J, Mathis D, et al. Stability of the regulatory T cell lineage in vivo. Science 2010;329(5999):1667–71.
[118] Jagger A, Shimojima Y, Goronzy JJ, Weyand CM. Regulatory T cells and the immune aging process: a mini-review. Gerontology 2014;60(2):130–7.
[119] Elderman M, van Beek A, Brandsma E, de Haan B, Savelkoul H, de Vos P, et al. Sex impacts Th1 cells, Tregs, and DCs in both intestinal and systemic immunity in a mouse strain and location-dependent manner. Biology of Sex Differences 2016;7(1):21.
[120] Lin P-Y, Sun L, Wierman M, Tekmal R, Pierce A, Daniel B, et al. Sex-related differences in regulatory T cell function are estrogen and B7-H1 dependent (143.53). The Journal of Immunology 2010;184(1 Supplement) 143.53-.53.
[121] Afshan G, Afzal N, Qureshi S. CD4+CD25(hi) regulatory T cells in healthy males and females mediate gender difference in the prevalence of autoimmune diseases. Clin Lab 2012;58(5-6):567–71.
[122] Garg SK, Delaney C, Toubai T, Ghosh A, Reddy P, Banerjee R, et al. Aging is associated with increased regulatory T-cell function. Aging Cell 2014;13(3):441–8.
[123] Darrigues J, van Meerwijk JPM, Romagnoli P. Age-Dependent Changes in Regulatory T Lymphocyte Development and Function: A Mini-Review. Gerontology 2018;64(1):28–35.
[124] Gregg R, Smith CM, Clark FJ, Dunnion D, Khan N, Chakraverty R, et al. The number of human peripheral blood CD4+ CD25high regulatory T cells increases with age. Clinical and experimental immunology 2005;140(3):540–6.
[125] Reitsema RD, Hid Cadena R, Nijhof SH, Abdulahad WH, Huitema MG, Paap D, et al. Effect of age and sex on immune checkpoint expression and kinetics in human T cells. Immunity & Ageing 2020;17(1):32.
[126] Klein SL, Morgan R. The impact of sex and gender on immunotherapy outcomes. Biology of sex differences 2020;11(1):24. -.
[127] Frydecka D, Misiak B, Pawlak-Adamska E, Karabon L, Tomkiewicz A, Sedlaczek P, et al. Sex differences in TGFB-β signaling with respect to age of onset and cognitive functioning in schizophrenia. Neuropsychiatr Dis Treat 2015;11:575–84.
[128] Krieglstein K, Miyazono K, ten Dijke P, Unsicker K. TGF-β in aging and disease. Cell and Tissue Research 2012;347(1):5–9.
[129] Shah TA, Rogers MB. Unanswered Questions Regarding Sex and BMP/TGF-β Signaling. J Dev Biol 2018;6(2):14.
[130] Okamoto Y, Gotoh Y, Uemura O, Tanaka S, Ando T, Nishida M. Age-dependent decrease in serum transforming growth factor (TGF)-beta 1 in healthy Japanese individuals; population study of serum TGF-beta 1 level in Japanese. Dis Markers 2005;21(2):71–4.
[131] Jenabian MA, Mehraj V, Costiniuk CT, Vyboh K, Kema I, Rollet K, et al. Influence of Hepatitis C Virus Sustained Virological Response on Immunosuppressive Tryptophan Catabolism in ART-Treated HIV/HCV Coinfected Patients. J Acquir Immune Defic Syndr 2016;71(3):254–62.
[132] Jenabian MA, Patel M, Kema I, Vyboh K, Kanagaratham C, Radzioch D, et al. Soluble CD40-ligand (sCD40L, sCD154) plays an immunosuppressive role via regulatory T cell expansion in HIV infection. Clin Exp Immunol 2014;178(1):102–11.
[133] Isnard S, Ramendra R, Dupuy FP, Lin J, Fombuena B, Kokinov N, et al. Plasma Levels of C-Type Lectin REG3alpha and Gut Damage in People With Human Immunodeficiency Virus. J Infect Dis 2020;221(1):110–21.
[134] Mehraj V, Ramendra R, Isnard S, Dupuy FP, Ponte R, Chen J, et al. Circulating (1−>3)-beta-D-glucan Is Associated With Immune Activation During Human Immunodeficiency Virus Infection. Clin Infect Dis 2020;70(2):232–41.